

MEASUREMENT OF VISCOSITIES OF SATURATED
METHANE-NONANE LIQUID MIXTURES
AT ELEVATED PRESSURES WITH
A CAPILLARY VISCOMETER

By

STUART EDWARD BENNETT

Professional Degree

Chemical and Petroleum Refining Engineering

Colorado School of Mines

Golden, Colorado

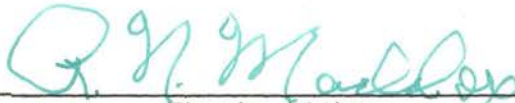
1966

Submitted to the faculty of the Graduate College
of the Oklahoma State University
in partial fulfillment of the requirements
for the degree of
MASTER OF SCIENCE
August, 1969

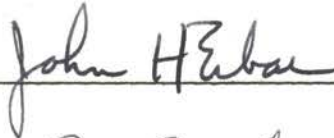
NOV 5 1969

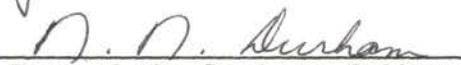
MEASUREMENT OF VISCOSITIES OF SATURATED
METHANE-NONANE LIQUID MIXTURES
AT ELEVATED PRESSURES WITH
A CAPILLARY VISCOMETER

Thesis Approved:



Thesis Adviser




Dean of the Graduate College

729859

PREFACE

The effect of viscosity on mass transfer rates in processes such as absorption has been recognized by the hydrocarbon processing industries. However, the behavior of viscosity under varying conditions of temperature, pressure, and composition is only partially understood. In particular, data and correlations are needed to more completely understand the change in viscosity with composition for typical hydrocarbon absorption process components. This study presents an examination of the viscosity changes of liquid methane-nonane mixtures at pressures up to 1200 psia and over a temperature range of -30°F to 78°F . The experimental apparatus built for the investigation used a Zeitfuchs style capillary viscometer installed in a pressure cell fitted with appropriate equipment to control operating conditions.

I am indebted to Prof. R. N. Maddox for the advice and assistance he has provided while serving as my research adviser for this project. I would also like to thank Prof. J. B. West for his assistance while serving on my thesis review committee and for his cooperation during my transfer from the University of Illinois. Also, my research associate, James R. Deam, deserves special mention and thanks for invaluable assistance and patience during this investigation.

The assistance of the OSU Research Apparatus Development Laboratory personnel during construction of the equipment is also recognized and appreciated.

I thank the Natural Gas Processors Association for providing funds to finance the purchase and construction of the experimental apparatus required in the investigation. The financial assistance provided by the School of Chemical Engineering of Oklahoma State University in the form of a research assistantship and the fellowship provided by the National Collegiate Athletic Association were greatly appreciated.

I especially wish to thank my wife, Kathy, and my parents, Mr. and Mrs. Edward E. Bennett, for their encouragement, confidence, and advice during my period of graduate study.

TABLE OF CONTENTS

Chapter	Page
I. INTRODUCTION	1
II. LITERATURE SURVEY	3
Historical Development	3
Previous Experimental Investigations	7
Viscosity Correlations	9
III. EXPERIMENTAL APPARATUS.	17
Materials Tested	18
Pressure Distribution System	18
Pressure Cell.	19
Liquid Injection System.	24
Viscometer	24
Temperature Controls	28
Lighting	30
IV. EXPERIMENTAL PROCEDURE.	31
System Preparation	31
Measurement.	33
Dismantling and Cleaning	34
V. RESULTS AND DISCUSSION OF RESULTS	35
Construction of Equipment.	35
Collection of Viscosity Data	37
Absolute Viscosity Behavior.	39
Surface-Tension Viscosity Correlation.	48
VI. CONCLUSIONS AND RECOMMENDATIONS	52
NOMENCLATURE.	57
A SELECTED BIBLIOGRAPHY	59
APPENDIX A - HEISE GAUGE CALIBRATION.	62
APPENDIX B - MEASUREMENT REPRODUCIBILITY.	64
APPENDIX C - VISCOMETER CALIBRATION	69
APPENDIX D - EXPERIMENTAL AND CALCULATED DATA	72
APPENDIX E - ANALYSIS OF ERRORS	80

LIST OF TABLES

Table	Page
I. Tabulated Viscosity Measurements	41
II. Least Squares Analysis for Surface Tension - Viscosity Correlation.	49
III. Heise Gauge Calibration.	63
IV. Study of Reproducibility of Viscometer Measurements	66
V. Viscometer Calibration	70
VI. Calculated Viscometer Constants.	71
VII. Experimental Flow Times.	73

LIST OF FIGURES

Figure		Page
1.	Schematic Diagram of Experimental Apparatus.	20
2.	Detail of Pressure Cell.	21
3.	Detail of Observation Port Assembly.	22
4.	Schematic Drawing of Liquid Injection System	25
5.	Zeitfuchs Style Viscometer	27
6.	Kinematic Viscosity of Methane-Nonane Bubble Point.	38
7.	Absolute Viscosity of Methane-Nonane Bubble Point Mixtures as a Function of Pressure	43
8.	Absolute Viscosity of Methane-Nonane Bubble Point Mixtures as a Function of Temperature.	44
9.	Absolute Viscosity of Methane-Nonane Bubble Point Mixtures as a Function of Composition.	45
10.	Absolute Viscosity of Methane-Nonane Bubble Point Mixtures as a Function of Density.	46
11.	Absolute Viscosity of Methane-Nonane Bubble Point Mixtures as a Function of Composition and Pressure	47
12.	Logarithm of Surface Tension as a Function of Reciprocal Viscosity for Methane-Nonane Mixtures	50
13.	Logarithm of Surface Tension as a Function of Reciprocal Viscosity for Methane-Butane Mixtures	51

CHAPTER I

INTRODUCTION

In September of 1964, Dr. James H. Weber of the University of Nebraska prepared a literature survey for the Natural Gas Processors Association (NGPA) which was entitled Factors Affecting Absorber Performance (34). On page 77 of the survey, Dr. Weber referred to the importance of viscosity in determining mass transfer rates which in turn affect tray efficiencies in absorbers.

In order to understand the effect of viscosity more completely, the Absorption Committee of NGPA desired viscosity data for typical absorption oil components. The particular information required by the NGPA was a determination of the change in viscosity of absorption oil components as the concentration of lighter hydrocarbons in the oil varied. Primary emphasis was to be placed on the study of binary liquid systems at equilibrium conditions. Measurements were to be conducted in a hydrocarbon gas atmosphere (methane) at pressures up to 1500 psia and over a temperature range of -50°F to 150°F .

In this study the following procedure was followed to obtain the required information.

1. An apparatus was built which used a capillary viscometer for obtaining viscosity data for the liquid phase of a binary hydrocarbon system (n-methane and n-nonane) at the required temperature and pressure conditions.
2. Experimental values of kinematic viscosity for the methane-n-nonane system over the required ranges of temperature and pressure were obtained with the apparatus.
3. The absolute viscosity was calculated from kinematic viscosity and its variations with temperature, pressure, and compositions were studied.
4. Absolute viscosity and surface tension were correlated.

CHAPTER II

LITERATURE SURVEY

Literature concerning this study of viscosity can be divided into three categories. One category encompasses the historical development of viscometry in general and the capillary viscometer in particular. The second category includes the experimental work that has been conducted either under high pressures or with hydrocarbon mixtures. The third category includes past attempts to correlate viscosity data. A discussion of the literature in all three categories is presented in this chapter.

Historical Development

The foundations of viscometry were established by Newton in the 1700's when he postulated his hypothesis of viscosity (21). Barr (1) presents the British Standards Institution interpretation of Newton's definition of the coefficient of viscosity."

"The coefficient of viscosity is the numerical value of the tangential force on a unit area of two parallel planes at a unit distance apart when the space between these planes is filled with the liquid in question and one of them moves with unit velocity in its own plane relatively to the other."

The mathematical expression of Newton's hypothesis as re-

ported by Barr is

$$F = \mu \frac{dv}{dx} \quad (1)$$

F = Force required

v = velocity of the plane

X = distance between planes

μ = dynamic or absolute viscosity

A quantity which also appears in the present viscosity study is the "kinematic viscosity," ν , equal to the dynamic viscosity divided by the density, ρ , of the fluid. The common unit of dynamic viscosity, μ , is called a poise in the cgs system ($\text{gm cm}^{-1} \text{sec}^{-1}$). The corresponding unit of kinematic viscosity is the stoke ($\text{cm}^2 \text{sec}^{-1}$).

Experimental capillary viscometry had its beginnings in the works of Hagen and Poiseuille in the mid 1800's. Barr(1) presents a detailed development of their work. Hagen's experiments consisted of the measurement of rates of discharge of water through tubes of 3, 4, and 6 mm. diam. as a function of temperature and pressure. In the mid 1840's, Poiseuille developed an expression describing the relationship between flow rate and pressure drop through a tube. Poiseuille did not refer to the viscosity of the fluid other than to recognize that the proportionality constant relating pressure drop and flow rate in his derivation was a particular value for a given liquid at a given temperature and pressure. Poiseuille's empirical relationship acquired the following form:

$$Q = k \frac{PD^4}{L} \quad (2)$$

Barr gives Weidemann credit for publishing one of the first theoretically derived versions of Poiseuille's law in 1856. Four years later, according to Barr, Hagenbach derived a more precise form of the relationship. The essential features of Hagenbach's original derivation have been retained in modern textbooks presenting a study of fluid flow in tubes (1, 3, 8, 33). Bird, et al(3) present the following result of the derivation which describes the flow of a liquid in a capillary

$$Q = \frac{\pi(\Delta P)r^4}{8\mu L} \quad (3)$$

Van Waser, et al(33) showed how the basic derivation of Poiseuille's law (3) can be expanded to allow its application to capillary viscometer measurements if one recognizes the following equivalences.

$$\Delta P = \rho g H$$

and

$$Q = \frac{V}{t}$$

If a kinetic energy correction term, ϵ , is introduced and Equation 3 is rearranged, the following expression results.

$$\mu = \frac{\pi r^4 \rho g H t}{8 L V} - \frac{\epsilon \rho V}{8 \pi L t} \quad (4)$$

Solving for the kinematic viscosity, ν , by dividing the absolute viscosity by the density, ρ , the following expression results.

$$\nu = \frac{\mu}{\rho} = \frac{\pi r^4 g H t}{8 L V} - \frac{\epsilon V}{8 \pi L t} \quad (5)$$

This equation is usually written

$$\nu = C_1 t - \frac{C_2}{t} \quad (6)$$

where C_1 is particular to a given viscometer, and the constant C_2 is reported by Van Wazer (33) to vary with the Reynolds's number of the fluid.

Johnson, et al (15) reported that numerical determination of C_2 is difficult. They felt that the best solution to the determination of C_2 would be to use a viscometer designed to make the constant C_2 as small as possible. The Zeitfuchs style viscometer (15, 35) was found to have a constant C_2 small enough to produce a kinetic energy correction ranging from 0.02% to 0.03%. Therefore, the corrections introduced by the kinetic energy term can be ignored for this viscometer and the simplified equation

$$\nu = C_1 t \quad (7)$$

may be used for viscosity determinations. The only information required for determination of C_1 is the value of t , which is determined by measuring the efflux time of a liquid of known viscosity. The value of C_1 can be calculated by Equation 7. The viscosity of a liquid of unknown viscosity may be obtained by measuring efflux time, t , and multiplying by the value of C_1 . Johnson, et al, also analyzed other sources of error that arise during viscosity measurements with the Zeitfuchs capillary viscometer. They maintained that the crossarm design of the viscometer virtually eliminated any errors caused by the differences in surface tension between the test liquid and calibrating liquid. Also,

the crossarm design eliminates errors resulting from liquid clinging to the walls of a bulb from which the liquid discharge is measured.

Previous Experimental Investigations

The following discussion of experimental viscosity studies of hydrocarbons and hydrocarbon mixtures is limited to that literature which has applicability to the conditions of the present investigation. Only studies of hydrocarbon viscosities at high pressures or of mixtures with characteristics similar to the methane-nonane system will be considered.

One of the first experimental studies of hydrocarbon mixture viscosities covering an extensive pressure and temperature range was reported in 1943 by Bicher and Katz (2). These investigators employed a rolling-ball inclined-tube viscometer to determine viscosities of methane, propane, and four of their binary mixtures (20, 40, 60 and 80 mole per cent methane). Viscosities were determined for pressures ranging from 400 to 5000 psia and temperatures from 77° F to 437° F.

In 1960 workers at the Institute of Gas Technology (IGT) published experimental viscosity data for liquid, gas, and dense fluid propane (31). The data, which were claimed to be accurate within $\pm 0.5\%$, were obtained with a capillary viscometer for pressures from 100 to 8000 psia for nine temperatures from 77° F to 280° F. In 1963 Dolan and coworkers(11)

continued the work by publishing viscosity data for n-butane. A comparison with existing experimental values showed agreement within $\pm 0.5\%$. The successful measurements achieved with this capillary instrument prompted Dolan, Ellington, and Lee (10) to undertake the study of methane-n-butane mixture viscosities. Their study covered a pressure range of 100 to 10,000 psia and temperatures from 100° F to 460° F. The method used to correlate the data is discussed later in this chapter.

In 1959 Reamer, Cokelet, and Sage (25) published information on the construction of a rotating cylinder viscometer and its use in determining viscosities of n-pentane. Later, Carmichael and his associates (6) used this viscometer to study viscosities of the methane-n-butane system previously examined by Dolan, Ellington, and Lee. Carmichael, et al, reported an average deviation from the IGT data of 1.1% for a mixture of 0.394 mole fraction methane. The comparison was made for temperatures of 100° F, 160° F, and 200° F and pressures of 1500 to 3000 psia.

Lee, Gonzalez, and Eakin (18) used the IGT viscometer to study the viscosities of liquid methane-n-decane mixtures. They presented tables of recommended viscosity values for temperatures from 100° F to 340° F and pressures from bubble point pressure to 7000 psia. The data were correlated using the concept of residual viscosity which is presented in the discussion of correlation methods later in this chapter. A maximum deviation of 3% was reported for a comparison

of correlated and experimental values.

Other studies of liquid binary hydrocarbon mixtures include the work of Heric and Brewer (14) who studied fourteen binary hydrocarbon mixtures and Katti and Chaudri (16) who presented data for binary systems of benzyl acetate, aniline, dioxane, and m-cresol. However, the preceding two investigations were conducted at atmospheric pressure and moderate temperatures (20°C to 40°C) and from the standpoint of the present investigation serve only to present a further understanding of viscosity behavior and correlation methods which may be applied to binary hydrocarbon systems.

Viscosity Correlations

One of the first recorded attempts to correlate viscosity was reported by Smith and Brown(30) to have been performed by Onnes in 1894. Onnes postulated that the following term has the same value for all substances in corresponding states:

$$\mu \left(\frac{T_c}{M^3 P_c^4} \right)^{1/6} \quad (8)$$

Smith and Brown pointed out that if reduced temperature and pressure were introduced, the following expression would result.

$$\frac{\mu}{\sqrt{M}} = f(T_R, P_R) \quad (9)$$

The same article by Smith and Brown cited a number of examiners who experimentally verified the preceding function.

In 1930, Nelson(20) plotted the viscosity of a number of

liquid and gaseous hydrocarbons against reduced pressure for a number of reduced temperatures. Nelson felt that plotting the ratio of the viscosity at given conditions to the viscosity at the critical point (ie., reduced viscosity) would have produced an improved relationship. However, the lack of critical point viscosity data at the time made such a correlation impossible.

Comings and Egly (5) also used a corresponding states approach in an attempt to correlate data for carbon dioxide, ammonia, nitrogen, and four light hydrocarbons. They plotted the ratio of the viscosity to the viscosity at 1 atmosphere against reduced pressure for lines of constant reduced temperature.

Smith and Brown(30) approached the problem by determining the limitations and values of the Onnes method. Onnes plotted η/η_c against T_R and P_R for data at 1 atmosphere. Smith and Brown determined that this plot predicted correct values for mixtures when the change of viscosity with concentration is linear. Smith and Brown replaced molecular weight by the molar average molecular weight and replaced reduced temperature and pressure by the pseudocritical properties. They reported that their correlation extended calculated viscosity data for paraffin mixtures in the range of pseudo reduced temperatures of 0.65 to 1.5 and reduced pressures up to 10.

In 1943 Bicher and Katz(2) used a method similar to that of Smith and Brown to correlate experimentally determined

viscosities of binary hydrocarbon mixtures. Bicher and Katz introduced a correction factor K and correlated $\eta/K\sqrt{M}$ with pseudoreduced temperature and pressure. K was found to be a function of molecular weight and was equal to unity for values of molecular weight greater than 32. Using experimental values of viscosity determined by other investigators, Bicher and Katz showed that their correlation produced an average deviation of 3.09 per cent. They emphasized that this correlation was good only for fluids in a single phase. Maximum deviation from experimental data occurred for values of pseudoreduced pressure between 0.8 and 1.2.

Another approach to the correlation problem was developed by Gonzalez and Bukacek(13). They used the basic method of Bicher and Katz but derived a method of calculating the molecular weight of the mixture from a momentum transfer approach. The momentum of a molecule of mixture is

$$M_m \bar{v}_m = \sum_{i=1}^n x_i M_i \bar{v}_i \quad (10)$$

From kinetic theory

$$T_m \propto M_m \bar{v}_m^2 \quad (11)$$

and

$$T_i \propto M_i \bar{v}_i^2 \quad (12)$$

If the proportionality constants of Equations 11 and 12 are equal and the temperatures are the same, the following expression is obtained.

$$\frac{\bar{v}_i}{\bar{v}_m} = \sqrt{\frac{M_m}{M_i}} \quad (13)$$

When Equation 13 is substituted into Equation 10 and then simplified, the following expression for mixture molecular weight results.

$$M_m = \left[\sum_{i=1}^n x_i \sqrt{M_i} \right]^2 \quad (14)$$

The data of Bicher and Katz were reproduced within 5% when viscosities were plotted against molecular weights calculated by the method of Equation 14. However, when applied to mixtures of dissimilar hydrocarbons (methane-n-decane mixtures), the method did not satisfactorily reproduce experimental data. Gonzalez and Bukacek felt that this discrepancy was caused by energy spent in the interaction of dissimilar molecules. Any accurate prediction of viscosity coefficients would have to consider this molecular shape effect.

Uyehara and Watson found that plotting the logarithm of the viscosities of gases at low pressure as ordinate against reduced temperatures yielded a family of curves. These curves may be superimposed by vertical translation corresponding to multiplication of the viscosities of each substance by a characteristic constant. The resulting curve accurately related the constant to T_R for all substances except highly polar materials. By combining this general reduced properties curve with the correlation of Comings and Egly, a relationship between reduced viscosity, $\mu_R = \frac{\mu}{\mu_c}$ and T_R and P_R resulted. Uyehara and Watson also presented a method of predicting critical viscosities based on an application of the method developed earlier by Onnes.

To predict mixture viscosities Uyehara and Watson

suggested using an extension of the pseudocritical concept introduced by Kay(17). That is, the viscosity of a mixture at its critical point is equal to the molal average of the critical viscosities of the components.

$$\mu_c = \mu_{c1} X_1 + \mu_{c2} X_2 + \dots \quad (15)$$

The viscosity of the mixture at temperature and pressure conditions other than the critical may then be predicted from the general curve of reduced viscosity. Uyehara and Watson claimed the same order of agreement as the Bicher and Katz correlations for the same hydrocarbon mixtures.

In 1958 Brebach and Thodos(4) introduced the concept of "residual viscosity," $\mu - \mu^*$, to eliminate temperature and pressure as variables in a study of diatomic gas viscosities. The residual viscosity represents the isothermal increase in viscosity due to pressure effects above one atmosphere. Brebach and Thodos compared residual viscosity and the viscosity at the critical point viscosity and developed a method to determine the critical point viscosity. The resulting value was utilized in plotting the reduced viscosity, μ_R , against reduced temperature, T_R . Curves for specific diatomic gases were obtained which were similar to the general curves developed by Uyehara and Watson(32). Although the curve developed by Brebach and Thodos for nitrogen predicted hydrogen and oxygen viscosities accurately, it could not be used to accurately predict the viscosities of polyatomic gases at high pressures. A comparison showed that for carbon dioxide, methane, and propane, use of the

Uyehara-Watson correlation predicted viscosity more accurately than the Brebach-Thodos curve for nitrogen.

In 1964 Dolan, Ellington, and Lee (10) described a method of correlating the viscosities of methane-n-butane mixtures by using the residual plot as developed by Thodos and Brebach. Since the method had been used with success by Thodos on pure components, Dolan, Ellington, and Lee expected that the data of a homogeneous mixture could also be correlated by using the residual plot. They found that the effects of changes in composition show regular trends between the limits of the two pure components which suggested the possibility of predicting viscosities by developing empirical mixing rules. However, they presented no such rules for high pressure systems.

In the last five years numerous authors have presented correlation methods based on Eyring rate theory (12). The general procedure followed by each set of investigators has been to apply simplifying assumptions to Equation 16, Eyring's equation, for the viscosity of pure liquids and develop constants particular to the system under study.

$$\mu = \left(\frac{\lambda}{\alpha}\right)^2 \frac{hN}{V} e^{f/RT} \quad (16)$$

Macedo and Litovitz (19) have considered both the rate-theory of Eyring and a free-volume approach to predicting liquid viscosities. They have arrived at a general correlation for predicting liquid viscosities and for studying the effect of free volume and intermolecular forces on the

transport properties of a fluid. Chaudri and Katti (16) interpreted data for binary mixtures of benzyl acetate, dioxane, aniline, and m-cresol by applying the Eyring relation for the viscosity of pure fluids. They assumed that molar free energies of activation of flow for two components are weighted according to mole fractions of the component with which they are associated. Also, for regular solutions they introduced the term W given by the following relation:

$$\frac{f_s}{RT} = x_1 \ln \frac{f_1}{RT} + x_2 \ln \frac{f_2}{RT} + x_1 x_2 \left(\frac{W}{RT} \right) \quad (17)$$

W is defined as the interaction energy for the activation of flow. The final expression for predicting viscosity is

$$\ln \mu \bar{V} = x_1 \ln \mu_1 \bar{V}_1 + x_2 \ln \mu_2 \bar{V}_2 + x_1 x_2 \frac{W}{RT} \quad (18)$$

Heric and Brewer (14) applied Equation 18 to binary hydrocarbon mixtures at atmospheric pressure and 25° C and achieved very good agreement between calculated and experimental values of viscosity.

Cullinan (7) provides a method for predicting mixture viscosities based on binary diffusion coefficients. The predictive equation derived appears as follows:

$$\mu = \mu_2 x_1 \mu_1 x_2 \frac{\bar{V}_A}{\bar{V}_G} \quad (19)$$

The article compared viscosities predicted by this equation with experimental binary hydrocarbon viscosity data found in the literature. No standard deviations or percent errors are presented, but the predicted values appeared to duplicate

experimental values in most cases. No comparisons were made for binary systems at elevated pressures.

An additional empirical predictive method has been developed by Pelofsky (22) and modified by Schonhorn (28). Pelofsky developed the following empirical relation between surface tension and viscosity.

$$\gamma = A e^{-B/\mu_L} \quad (20)$$

Pelofsky tested his equation on a number of pure components and liquid solutions with success. Schonhorn extended the equation by subtracting the vapor viscosity from the liquid viscosity in the exponential term. He stated that this modification has the effect of extending the temperature range for which the correlation is valid.

CHAPTER III

EXPERIMENTAL APPARATUS

In order to use the glass capillary viscometer at high static pressures, the experimental apparatus had to be built so that there was never any large pressure drop across the viscometer. At the same time facilities had to be provided to induce small pressure differences to control liquid position in the viscometer. The equipment was also designed to allow repeated viscosity measurements at one set of temperature and pressure conditions without requiring a new liquid sample for each measurement. Appendix B describes the tests used and data obtained to verify the accuracy of repeated measurements on the same liquid sample. A schematic diagram of the equipment used in this investigation is shown in Figure 1.

The primary elements of the equipment are the viscometer, the pressure cell, the constant temperature bath, and the flow system used to introduce methane to the viscometer. The construction and function of these components and a description of the hydrocarbons tested is described in the following discussion.

Materials Tested

The methane used was Phillips Petroleum Company instrument grade guaranteed to be at least 99.05 mole per cent methane. The nonane used was Phillips Petroleum Company research grade guaranteed to be 99.65 mole per cent n-nonane.

Pressure Distribution System

The pressure distribution system had the functions of introducing the methane to the viscometer, controlling the level of the liquid in the viscometer reservoir, and achieving fine control of the system pressure. The pressure distribution system may be discussed in terms of its contributions to the achievement of these functions.

Methane gas was introduced to the system from a methane cylinder via a Matheson pressure regulator which also helped control the system pressure. Valving was arranged to allow methane to be passed through the system by any desired route. Pressure was measured by a Heise Bourdon-tube pressure gauge. The gauge had a 12 in. diam. face graduated in 5 psia increments up to 3000 psia. Tubing for the system was 1/8 in. O.D. by 0.06 I.D. type 316 stainless steel tubing. Valves employed were type 316 stainless steel Whitey O-series valves. All unions, connectors, and tees were either standard Autoclave or Swagelok fittings.

Control of the pressure on the system was achieved by operation of the vent valve and the inline pressure con-

troller consisting of a modified portion of hydraulic pressure generator system composed of a cylinder, piston, and a screw-drive which controlled the height of the piston in the cylinder. A pressure-tight seal was achieved by means of two Viton O-rings set in grooves on the piston wall so they were in contact with the polished surface of the cylinder wall. Operation of the screw drive changed the volume of the cylinder space below the piston thereby changing the volume of the pressure system. Small changes in system volume were used to control liquid levels in the viscometer.

Evacuation of the system atmosphere was accomplished by employing a model 1403 Duo-seal vacuum pump with a rated capability of producing a pressure of 5 microns in the system.

Pressure Cell

The pressure cell (Fig. 1) had the functions of maintaining pressure on the viscometer while allowing direct observation of the liquid flow through the viscometer. Components were the main cell body and the observation ports.

The cell body (Fig. 2) was constructed from a 14-1/2 in. long by 8 in. O.D. type 304 stainless steel cylinder. Space for the viscometer was provided by one 12-1/2 in. deep by 2-3/4 in. diam. hole bored concentric to the cylinder. A 4-1/8 in. I.D. by 3/16 in. thick Viton O-ring provided the seal between the main cell cylinder and a 1-5/8 in. thick type 304 stainless steel flange. Eight 5/8 in. diam.

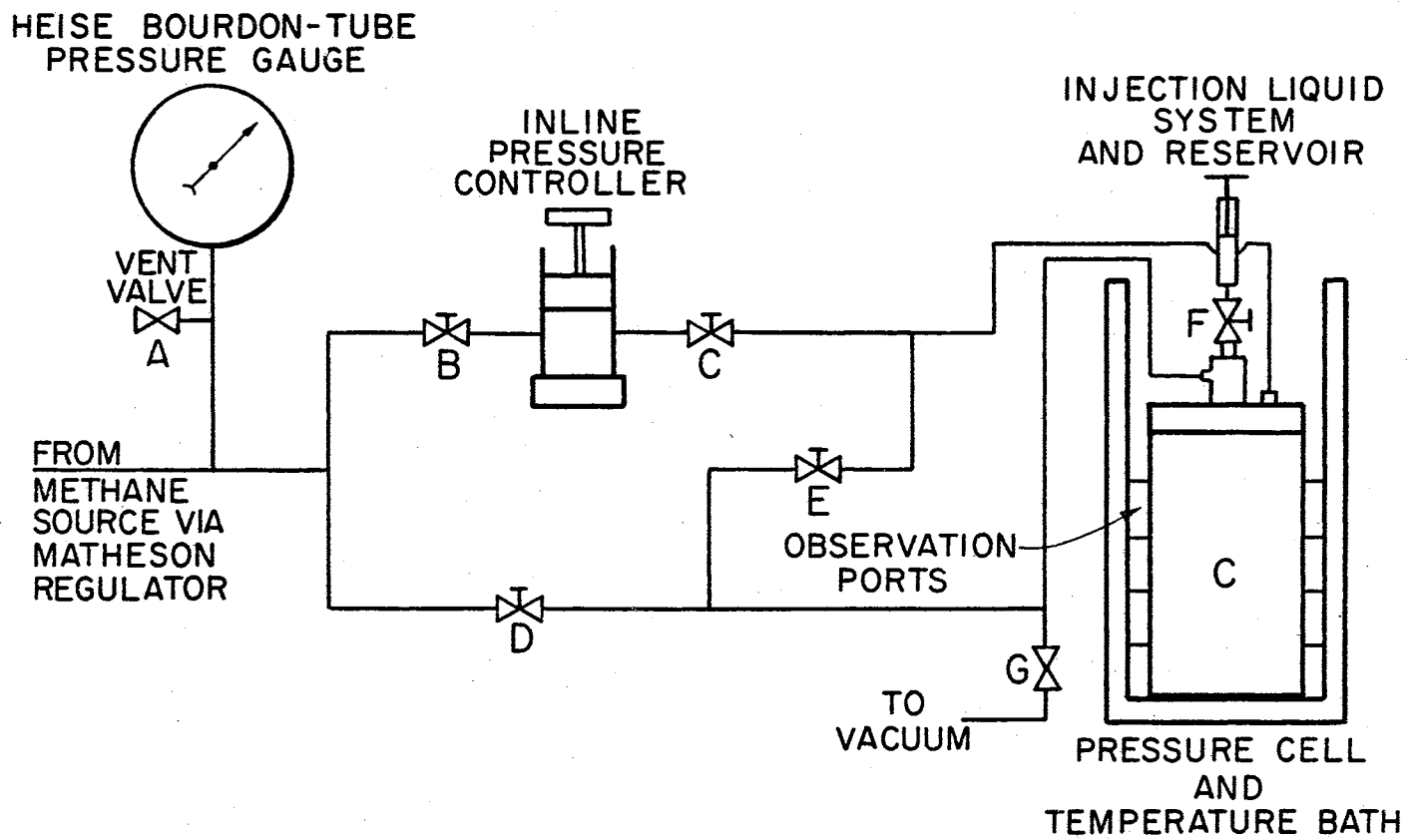


Figure 1. Schematic Diagram of the Experimental Apparatus

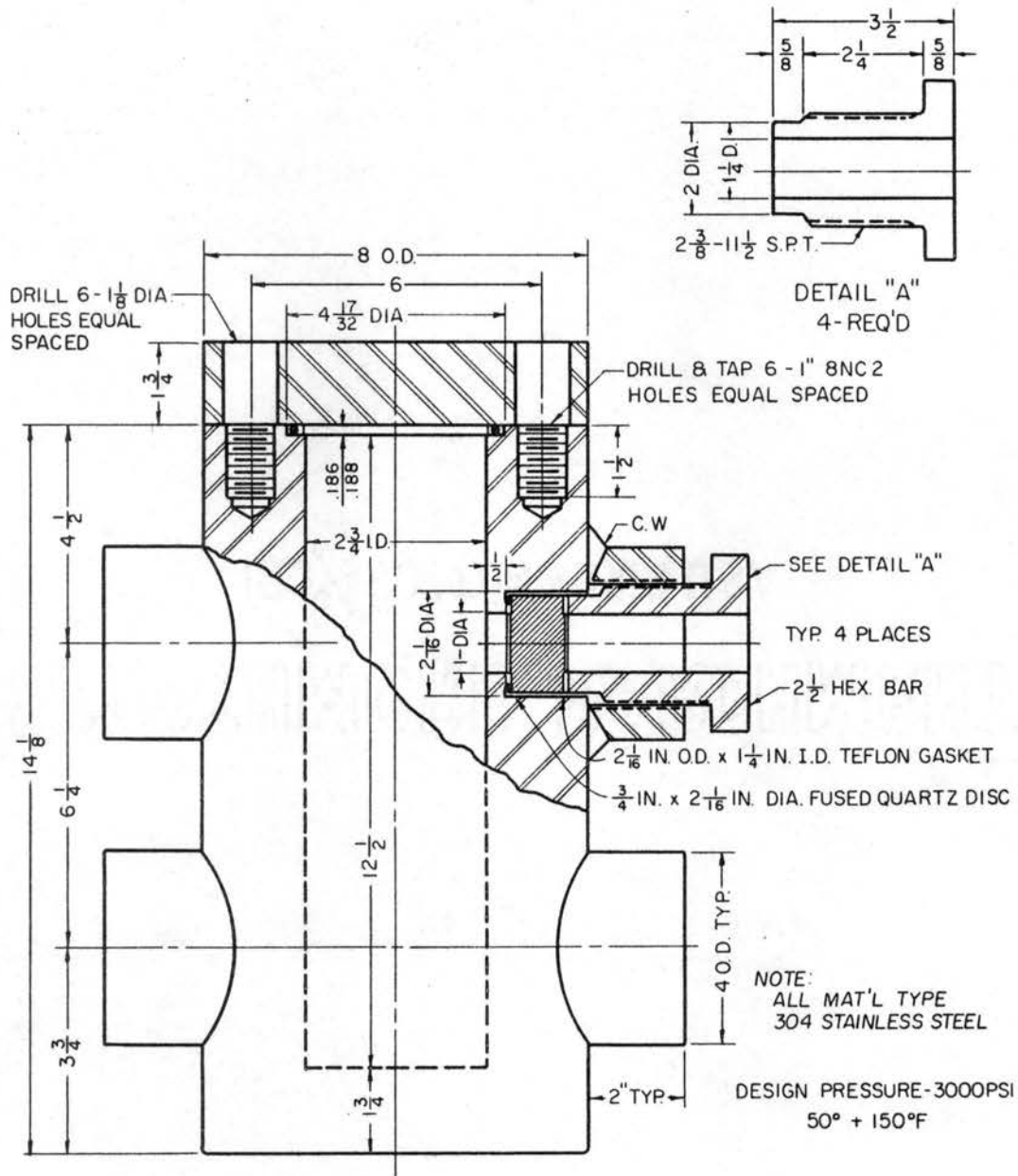


Figure 2. Detail of Pressure Cell

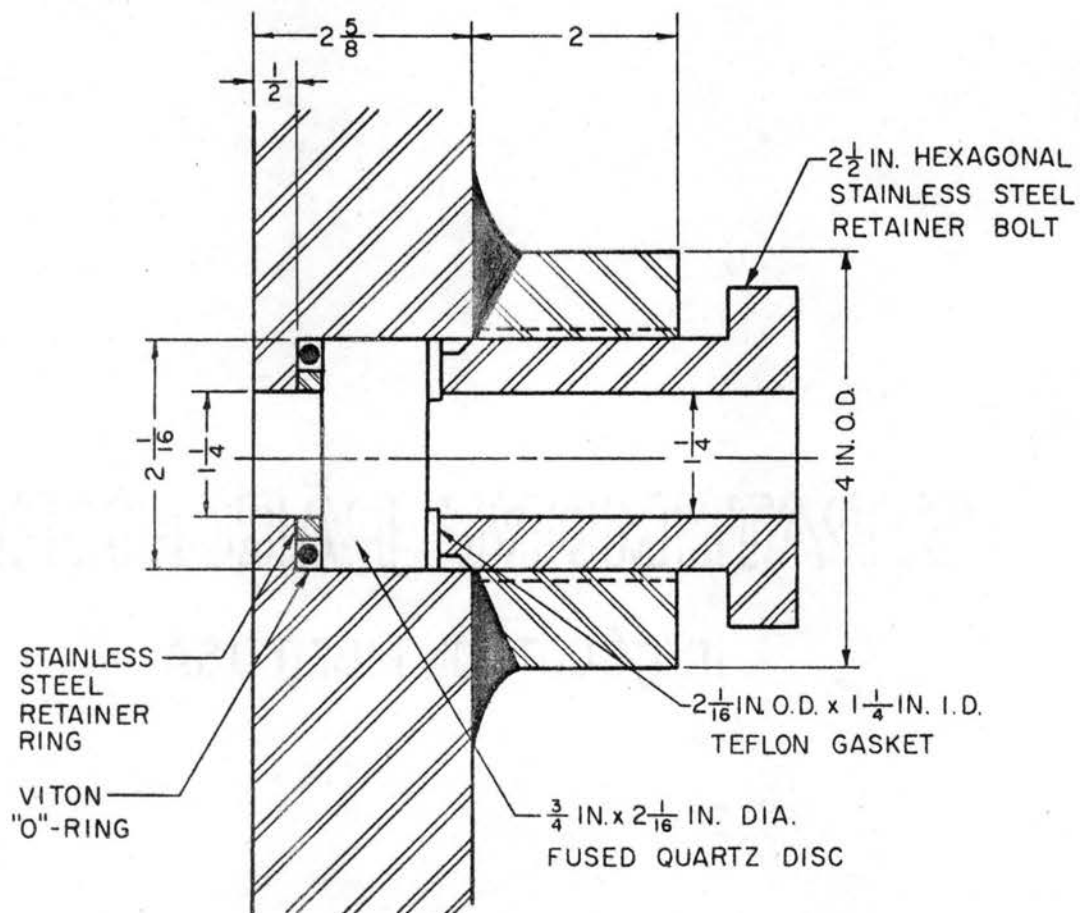


Figure 3. Detail of the Observation Port Assembly

cadmium-plated stainless steel bolts anchored the flange to the cell body.

Four 1-1/4 in. diam. observation ports were installed on the sides of the cell. The placement of the ports is indicated in Figure 2. The outer wall of each port was machined from a 4 in. diam. type 304 stainless steel cylinder bored and threaded to an inner diameter of 2 in. and welded to the cell body. Figure 3 illustrates assembly of the ports. The optical medium in the ports is a 2-1/6 in. diam. by 3/4 in. thick fused quartz lens constructed by the General Electric Company Lamp Glass Department. With a thickness to unsupported diameter ratio of 0.6, the lenses were capable of service up to 2200 psia with a safety factor of 7 to 1. The seal between the quartz lens and the pressure cell was achieved by a 1.56 in. I.D. by a 0.21 in. thick Viton O-ring. A stainless steel ring placed inside the O-ring and concentric to it prevented the O-ring from collapsing when the cell was evacuated. A 1/16 in. thick, 2-1/16 in. O.D. by 1-1/4 in. I.D. Teflon ring was then placed in the port against the quartz lens. The lens, O-ring, Teflon ring assembly was held in place by a 2 in. O.D. by 1-1/4 in. I.D. cadmium-plated 304 stainless steel bolt machined from 2-1/2 in. hexagonal bar. The bolt was tightened by hand to hold the entire lens assembly in place. The pressure seal was achieved by the O-ring and not by tightening the retainer bolt. If the bolt were pulled too tight, weakening of the lens because of scratching could occur. Because of the

potential danger of lens breakage, observation was indirect by a mirror focused on the observation ports.

Liquid Injection System

The liquid injection system (Fig. 4) contained the nonane test liquid. The piston in the injection system provided a method of controlling the amount of liquid introduced to the viscometer. The system was composed of a liquid reservoir cylinder, an injection piston, a ball valve, a methane gas inlet, and a tube for introducing nonane to the viscometer.

The reservoir cylinder and piston were constructed from type 316 stainless steel. The piston O.D. and cylinder I.D. are 1/2 in. Walls of the cylinder were 3/32 in. thick. A volume of about 12 cc. of nonane was retained in the cylinder. A Viton O-ring set in a circumferential groove cut on the piston surface created the pressure seal. The cylinder was threaded to fit a 1/4 in. NPT female tap.

A Hoke ball valve was attached to the reservoir cylinder by a hexagonal brass union brazed to the valve body. The valve served to trap the nonane sample in the reservoir cylinder.

Viscometer

The capillary viscometer served as the measuring device for this investigation. The viscometer used was a model C-50 Zeitfuchs cross-arm viscometer manufactured by the Calif-

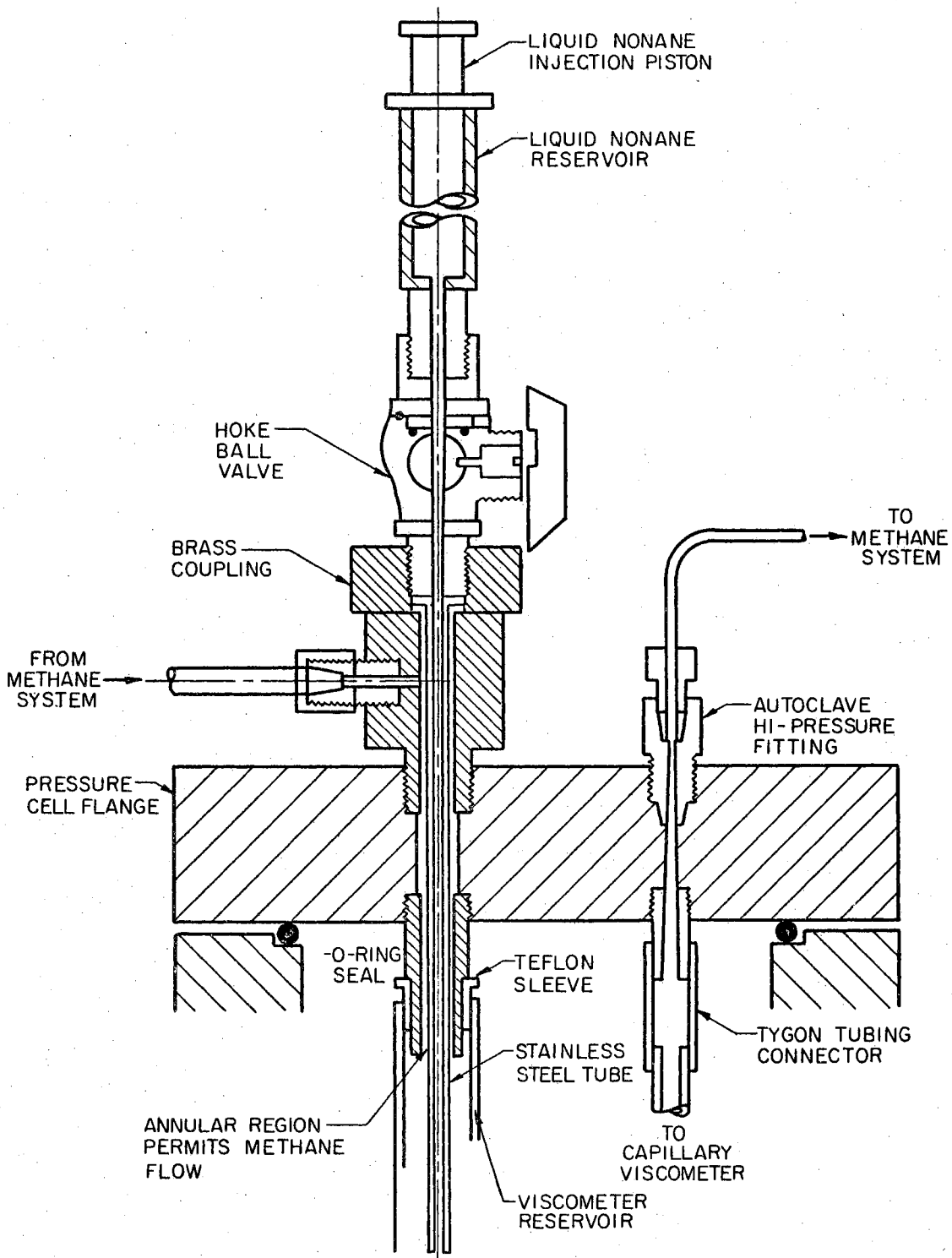


Figure 4. Schematic Drawing of Liquid Injection System

ornia Laboratory Equipment Company (Fig. 5). A detailed description of the viscometer was published by Johnson, LeTourneau, and Matteson(14). The components of the viscometer are the reservoir, cross-arm, capillary tube, and bracing.

The reservoir served to hold the liquid sample and the cross-arm allowed passage of the sample from the reservoir to the capillary tube. Lines scribed on the reservoir and cross-arm walls provided an accurate method of introducing a consistent size sample to the viscometer. Measurement of viscosity was conducted in the U-tube capillary in which a bulb was located to allow measurement of flow times. As the liquid sample passed through the capillary and into the bulb, the passage of the meniscus between scribed lines on the bulb wall was timed. The viscometer was mounted in a chrome-plated brass head which served to support the viscometer in the pressure cell.

The viscometer was connected to the liquid injector and methane feed lines by a Teflon sleeve which fit tightly against the walls of the reservoir and a 1 in. length of Tygon tubing which fit tightly over the capillary end of the viscometer (Fig. 4). A wingnut held the viscometer at the correct level on the sleeve. Slots cut longitudinally in the Teflon sleeve allowed gas to escape from the viscometer reservoir to the pressure cell and maintained the interior and exterior of the viscometer at the same pressure.

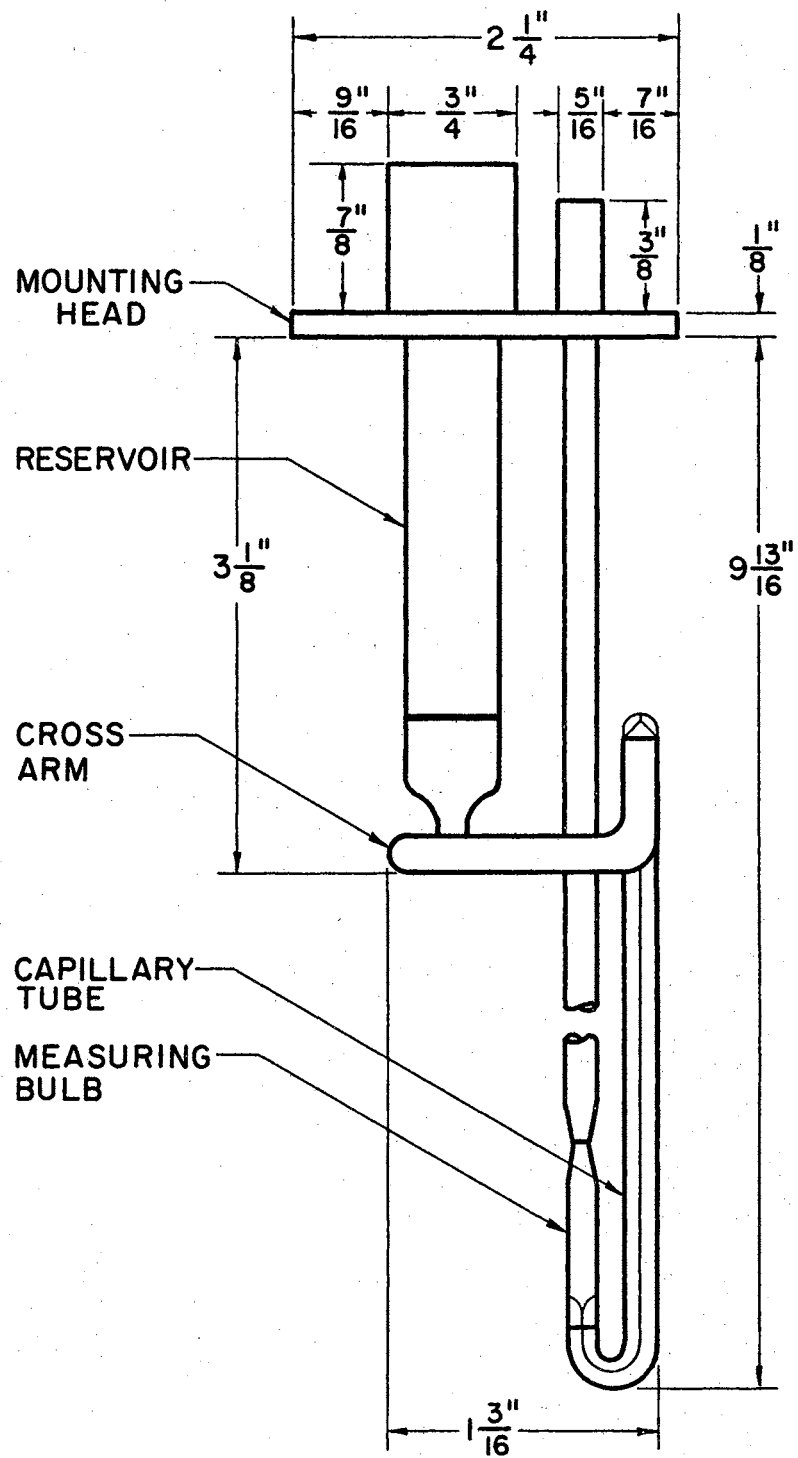


Figure 5. Zeitfuchs Style Viscometer

Temperature Controls

Apparatus for controlling system temperature was composed of the temperature bath, the refrigeration system, and the temperature controller.

The temperature bath was constructed by the OSU Research Apparatus Development Lab. The bath was composed of two stainless steel boxes one of which was 1 in. smaller in dimensions and was placed inside the larger box. The dimensions of the inner box were 24 in. by 11 in. by 8-1/2 in. Aluminum frames 1/2 in. thick were placed between the walls to maintain a 1/2 in. space between the inside and outside walls of the bath. "Peco-foam" was placed in the remaining spaces between the walls to assist in insulating the system.

A primary requirement of the bath was to keep the pressure cell immersed in liquid but still permit the observation ports to remain unobstructed either by coolant or walls. To achieve this function, a 22 in. by 7 in. section was cut from one of the 24 in. by 11 in. walls. The resulting exposure of the inner and outer walls was filled with a 1/2 in. thick U-shaped aluminum frame bolted to the walls and sealed with a silicone sealer. In the remaining 24 in. by 11 in. wall, two 4-1/4 in. holes were cut to allow the observation ports to project through the wall. An O-ring seal was used to create a liquid tight seal around the ports. A stainless steel door which also was provided with the O-ring sealed holes for the observation ports was

bolted over the section which had previously been removed. A rubber gasket was placed between the bolted on door and the bath walls. The resulting assembly allowed the four observation ports of the pressure cell to project through the bath walls so the quartz lenses were not obscured by any portion of the bath or its coolant.

The finished bath was coated on the inside with an epoxy to insure that there would be no leaks. Fibreglass insulation was placed around the finished bath and an insulated lid was fabricated to cover the top opening.

The refrigeration system used was a compression unit constructed by the OSU refrigeration department. Freon 22 was used to cool methanol which was employed as the coolant for the experimental apparatus. Methanol was pumped by an Eastern Industries Model D11 centrifugal pump from the refrigeration system to the temperature bath through 1/2 in. diam. copper tubing insulated with Armstrong Armaflex insulation. Coolant was returned to the refrigeration system via an Eastern Industries model D 6 centrifugal pump. Circulation within the bath was improved by using a "Jumbo Stirrer" obtained from Fisher Scientific Co.

Because of the large mass of the pressure cell and bath, once the desired system temperature was reached there was little difficulty in maintaining it. However, fine control was achieved by an immersion heater connected to a Thermistemp Model 63 temperature controller which operated between -40° F and 120° F and was capable of controlling

temperatures to $\pm 0.1^{\circ}$ F. When operating at temperatures above room temperature, the bath was isolated from the refrigeration system and tap water was used in the bath instead of methanol.

Lighting

The viscometer measuring bulb was illuminated by a high intensity Anvil model 4975 lamp placed so that light showed through the cell toward the observer. Additional illumination was provided by a fluorescent light placed behind the cell.

CHAPTER IV

EXPERIMENTAL PROCEDURE

The experimental procedure may be divided into the three following operations: system preparation, measurement, and dismantling and cleaning. Schematic location of valves and other equipment discussed may be found in Figure 1.

System Preparation

To introduce the liquid n-nonane sample to the level controller, the ball valve (F) was closed and the piston of the level controller was removed. About 12 cc. of n-nonane was transferred directly from the storage bottle to the reservoir cylinder. After replacing the piston the injection system flange-viscometer assembly was placed into the pressure cell and fastened securely against the O-ring seal. Lines from the gas flow system were then attached to the viscometer assembly. After all valves except the vent valve (A) and ball valve (F) were opened, the vacuum pump was started and the system was evacuated to a pressure of 25 microns and the valve (G) closed. The coolant liquid or heater liquid was introduced to the temperature bath and temperature controls were adjusted for the desired experimental conditions.

Methane was introduced to the system by opening the Matheson regulator and admitting methane until a pressure of about 50 psia registered on the pressure gauge. When this pressure was obtained, the methane regulator was closed and the ball valve (F) was opened. The viscometer reservoir was then filled to the hairline marks with nonane by depressing the piston of the liquid level control system after which the valve (F) was again closed. Valves (D) and (E) were then closed and methane flow was resumed. The closed valves forced the methane to bubble through the n-nonane in the viscometer reservoir to achieve mixing and aid in reaching phase equilibrium. Methane was introduced to the system slowly to assist in reaching equilibrium. When the desired system pressure was reached, the methane source was again isolated. The apparatus was allowed to remain idle for 30 minutes after the desired temperature and pressure were reached. During this time, methane was bubbled through the liquid mixture by manipulation of the inline pressure controller. Equilibrium was assumed achieved when consistent measurements over a 30 minute period were obtained.

When measurements were to be made at temperatures below 32^oF, the methane was introduced to the system and the desired pressure obtained before the pressure cell was cooled. A pressure change at low temperatures had a tendency to cause leaks around O-ring seals because the O-rings became rigid and had inadequate flexibility to maintain the seal.

Measurement

Since the pressure line from the inline pressure controller was fastened directly to the viscometer by a tight fitting Tygon tube, any change in volume of the pressure controller created a slight pressure difference across the viscometer. The level of the liquid sample in the viscometer reservoir was controlled by manipulation of the pressure controller piston.

A measurement run was initiated by opening valve (D) and increasing the volume in the pressure controller until liquid began flowing through the viscometer capillary. The flow of liquid past the hairlines on the viscometer was observed through the lower observation ports and the time required for the liquid to pass the hairlines was recorded.

As the phase rule

$$f = c - p + 2$$

f = degrees of freedom

p = phases

c = components

predicts, the composition of the liquid is fixed as a bubble point liquid. The system contained two components in two phases which allowed two degrees of freedom--temperature and pressure--and dictated all other factors including composition.

To repeat a measurement, the valve (D) was again closed and the inline controller depressed to force the liquid

back up the capillary and into the viscometer reservoir. Procedures for a viscosity measurement were then repeated. Flow times were not recorded until the second measuring procedure to insure that the bulb walls were wetted and the calibrated viscometer constant was valid. Achievement of equilibrium was assumed when reproducible times for a set of conditions were obtained.

Dismantling and Cleaning

To dismantle the equipment after a series of measurements had been obtained, valve (C) was closed, ball valve (F) was opened, and vent valve (A) was opened. The pressure difference created allowed all liquid n-nonane (which had been under pressure) to flow to the viscometer reservoir. Also, the pressure difference prevented the nonane from being sucked through the pressure controller. Coolant was then pumped out of the temperature bath to permit access to the flange assembly.

After the system was reduced to atmospheric pressure, the controller-flange-viscometer assembly was removed from the pressure cell. The viscometer was removed from the assembly, flushed with acetone, and dried with a stream of filtered air.

CHAPTER V

RESULTS AND DISCUSSION OF RESULTS

The results of this investigation were studied in terms of the objectives presented in Chapter I. In summary, these objectives were a) construction of equipment suitable for obtaining kinematic viscosity data, b) collection of viscosity data, c) investigation of the behavior of calculated absolute viscosity as system variables were changed, and d) an attempt to correlate surface tension and absolute viscosity data.

Construction of Equipment

Details of construction and operation of the equipment have been presented in Chapters III and IV, respectively. Because measurements were to be obtained visually while the system was under pressure, the observation ports described in Chapter III were designed. These ports provided leak-tight seals and provided adequate observation of the capillary viscometer in the pressure cell.

In order to eliminate the need of reaching new equilibrium conditions for each viscosity measurement, a liquid mixture at a given temperature and pressure was measured repeatedly by controlling the position of the liquid in the

capillary viscometer. Before the repeated measurement procedure could be used, an investigation was conducted to determine if measurements obtained in this manner were reproducible. Data associated with this investigation are presented in Appendix B. A number of flow measurements were conducted individually. That is, the viscometer was cleaned and dried after each flow measurement. Each measurement was obtained with a fresh liquid sample of distilled water. Flow times obtained in the preceding manner were compared with flow times obtained by repeated measurement of the flow time of one distilled water sample. The values obtained by each method did not differ significantly. However, for repeated measurements the viscometer constant had to be changed to obtain accurate results. Appendix B indicates the reproducibility of measurements obtained by each procedure.

Zeitfuchs capillary viscometers with cell constants reported by the manufacturer to be 0.01 and 0.003 were calibrated with distilled water (see Appendix C). The 0.003 constant viscometers were initially installed in the pressure cell because the reproducibility of flow times taken with these viscometers was better than measurements taken with a 0.01 viscometer. However, when the viscometer was placed inside the pressure cell the flowing liquid sample in the viscometer capillary was difficult to see. The viscometer with the 0.01 reported constant and thus, the larger capillary, was then installed in the cell and found to permit

observation of the flowing liquid. Therefore, even though some reproducibility was apparently sacrificed, use of the 0.01 viscometer allowed greater ease in obtaining viscosity measurements.

With better illumination the 0.003 constant viscometer could possibly be used which would initiate a corresponding increase in reproducibility.

Collection of Viscosity Data

The experimental procedure outlined in Chapter IV was followed to obtain measurements of kinematic viscosity and fulfill the second objective of this investigation. Flow times of liquid samples were recorded for a temperature range of -30° F to 78° F and a pressure range of 150 psia to 1200 psia. The flow times and percentage deviation from the average time for the controlled temperature-pressure conditions are presented in Appendix D. The largest recorded percent deviation from the average was 5.2 per cent. Most of the times fell well within a deviation of one percent from the average time. Values of kinematic viscosity were obtained by multiplying the flow times by the cell constant of the viscometer. Figure 6 presents isotherms of the calculated kinematic viscosities plotted as a function of pressure. The general trends indicated in the graph are that viscosity decreases as pressure increases at constant temperature and viscosity increases as temperature decreases at constant pressure.

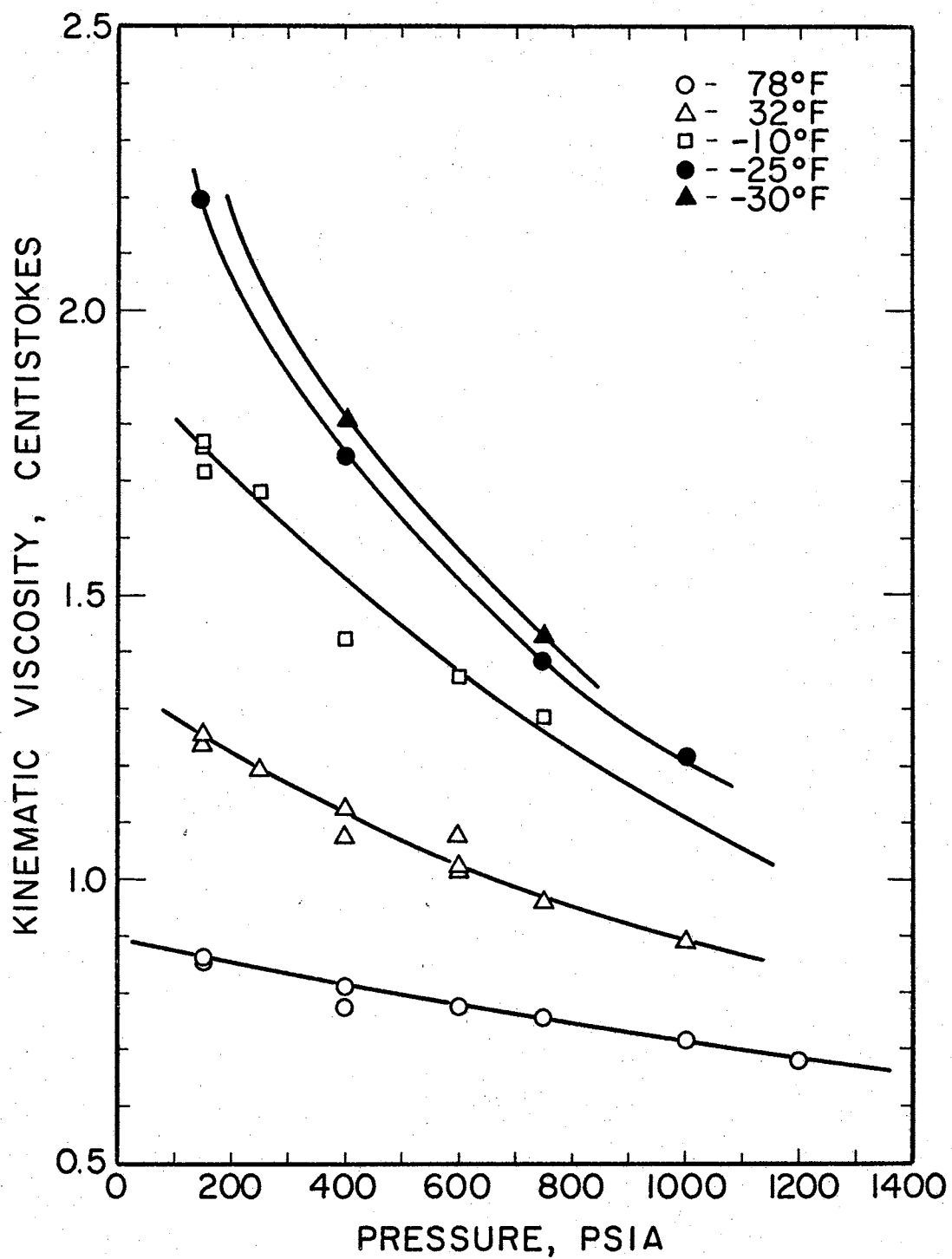


Figure 6. Kinematic Viscosity of Methane-Nonane Bubble Point Mixtures at Constant Temperatures

Absolute Viscosity Behavior

The third objective of this investigation was the calculation of absolute viscosity values and analysis of the effect of system variables on viscosity behavior. Values of kinematic viscosity were multiplied by the density of the mixture to obtain absolute viscosity. Densities and compositions of the methane-nonane system were interpolated from the data of Shipman and Kohn(26). Absolute viscosities calculated and the corresponding properties of the mixture are presented in Table I. Experimental data has been plotted in Figures 7 through 11.

Isotherms of absolute viscosity showed a variation with pressure similar to the behavior of kinematic viscosity. That is, absolute viscosity decreased as pressure increased at constant temperature (see Figure 7) and absolute viscosity increased as temperature decreased at constant pressure (see Figure 8). Figure 9 indicates the changes in absolute viscosity as the composition of the liquid mixture varied. As the percentage of methane in the liquid was increased at constant temperature, the absolute viscosity decreased. The change of absolute viscosity as the density changed is shown in Figure 10. For isothermal absolute viscosity measurements, Figure 10 shows that an increase in density created an increase in absolute viscosity.

A three dimensional plot of composition and pressure and absolute viscosity for constant temperatures is shown in

Figure 11. For constant pressures, an increase in the methane composition of the mixture causes an increase in the absolute viscosity. However, in order to increase the methane composition in the system the temperature must decrease. One may also note that for an increase in pressure at constant composition, viscosity decreases and temperature increases.

Through examination of the trends of Figures 7, 8, 9, and 11, one notices that for a bubble point mixture a) the effects of a temperature decrease override the effects of a methane composition increase and, b) the effects of a temperature increase are greater than a pressure increase. Therefore, one may conclude that the significance of temperature change is greater than either composition or pressure change in this bubble-point system.

TABLE I

TABULATED VISCOSITY MEASUREMENTS

<u>T OF</u>	<u>P, PSIA</u>	<u>T, SEC</u>	<u>DENSITY, GM/ML*</u>	<u>KINEMATIC VISCOSITY</u>	<u>ABSOLUTE VISCOSITY</u>	<u>METHANE* FRACT</u>	
78	150	78.4	0.7042	0.8624	0.6073	0.052	
	150	78.2	0.7042	0.8602	0.6052	0.052	
	400	70.7	0.6961	0.7777	0.5181	0.1306	
	400	73.8	0.6961	0.8118	0.5649	0.1306	
	600	70.8	0.6893	0.7788	0.5367	0.186	
	750	68.97	0.6842	0.7590	0.5194	0.2245	
	1000	65.3	0.6750	0.7183	0.4845	0.2790	
	1200	61.98	0.6660	0.6818	0.4541	0.3211	
	32	150	114.0	0.7251	1.2540	0.9093	0.055
			112.3	0.7251	1.2353	0.8957	0.055
250		108.5	0.7220	1.1930	0.8613	0.0895	
400		97.97	0.7157	1.0777	0.7713	0.1419	
		102.9	0.7157	1.1319	0.8101	0.1419	
		102.2	0.7157	1.1242	0.8046	0.1419	
		101.98	0.7157	1.1218	0.8029	0.1419	
600		92.4	0.7067	1.0164	0.7183	0.2041	
		93.07	0.7067	1.0238	0.7235	0.2041	
750		87.54	0.6998	0.9629	0.6738	0.2494	
1000	81.77	0.6885	0.8999	0.6169	0.3263		
-10	150	155.97	0.7412	1.7157	1.2463	0.0657	
		160.7	0.7412	1.7677	1.3102	0.0657	
		159.16	0.7412	1.7507	1.2976	0.0657	
	250	152.8	0.7347	1.6808	1.2349	0.1066	
	400	129.6	0.7303	1.4256	1.0411	0.1577	
	600	123.35	0.7160	1.3568	0.9714	0.2316	
	750	117.2	0.7104	1.2892	0.9158	0.2772	
-25	150	199.62	0.7464	2.1958	1.6389	0.0887	
	400	158.4	0.7329	1.7424	1.2770	0.1831	

*Interpolated from data of Shipman and Kohn (29).

TABLE I (continued)

TABULATED VISCOSITY MEASUREMENTS

<u>T °F</u>	<u>P, PSIA</u>	<u>T, SEC</u>	<u>DENSITY, GM/ML*</u>	<u>KINEMATIC VISCOSITY</u>	<u>ABSOLUTE VISCOSITY</u>	<u>METHANE* FRACT</u>
	750	125.9	0.7124	1.3845	0.9863	0.3099
	1000	110.08	0.7007	1.21088	0.8485	0.3823
-30	150					0.0969
	400	164.32	0.7339	1.8075	1.3265	0.1890
	750	130.08	0.7129	1.4309	1.0201	0.3178

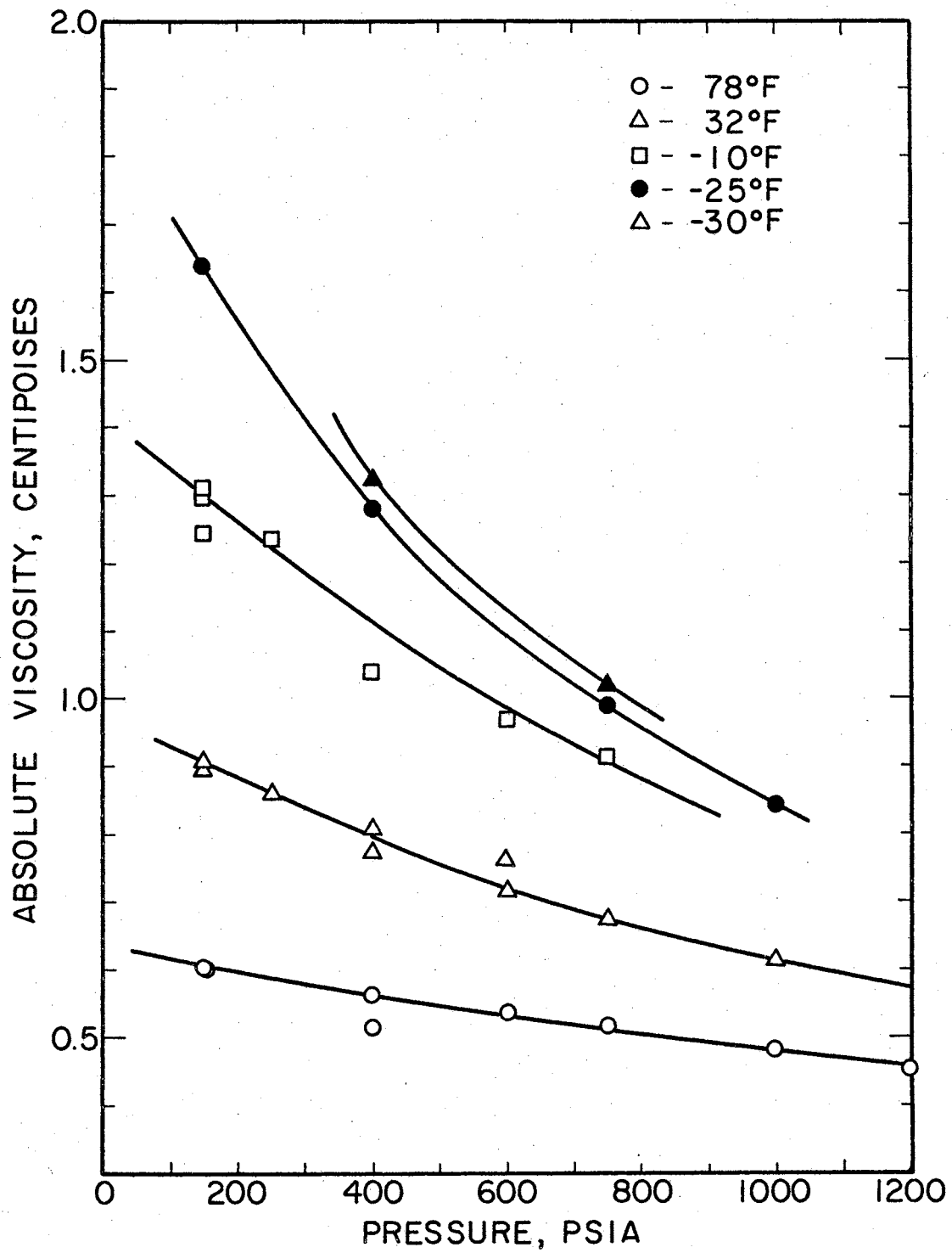


Figure 7. Absolute Viscosity of Methane-Nonane Bubble Point Mixtures as a Function of Temperature

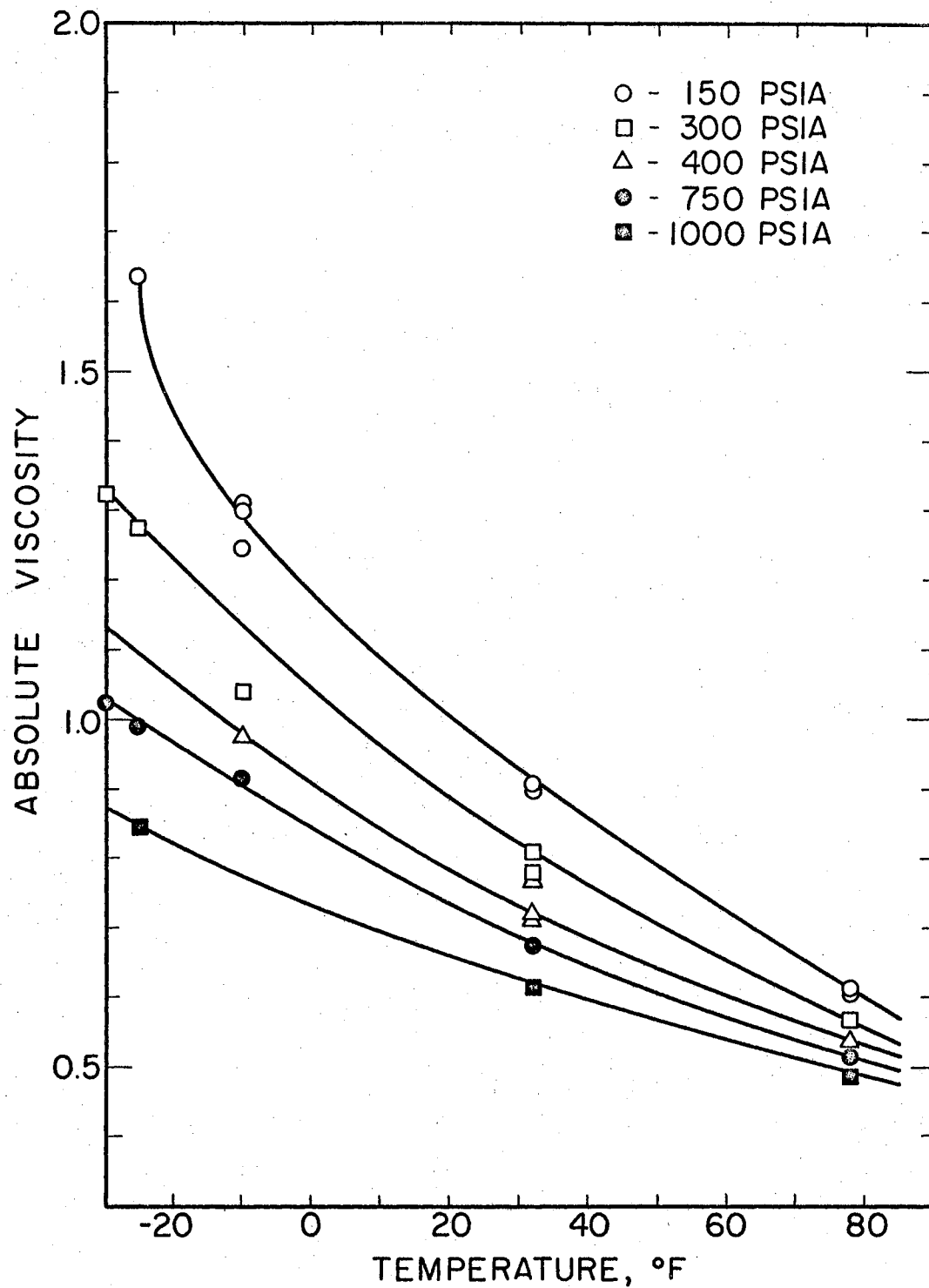


Figure 8. Absolute Viscosity of Methane-Nonane Bubble Point Mixtures as a Function of Temperature

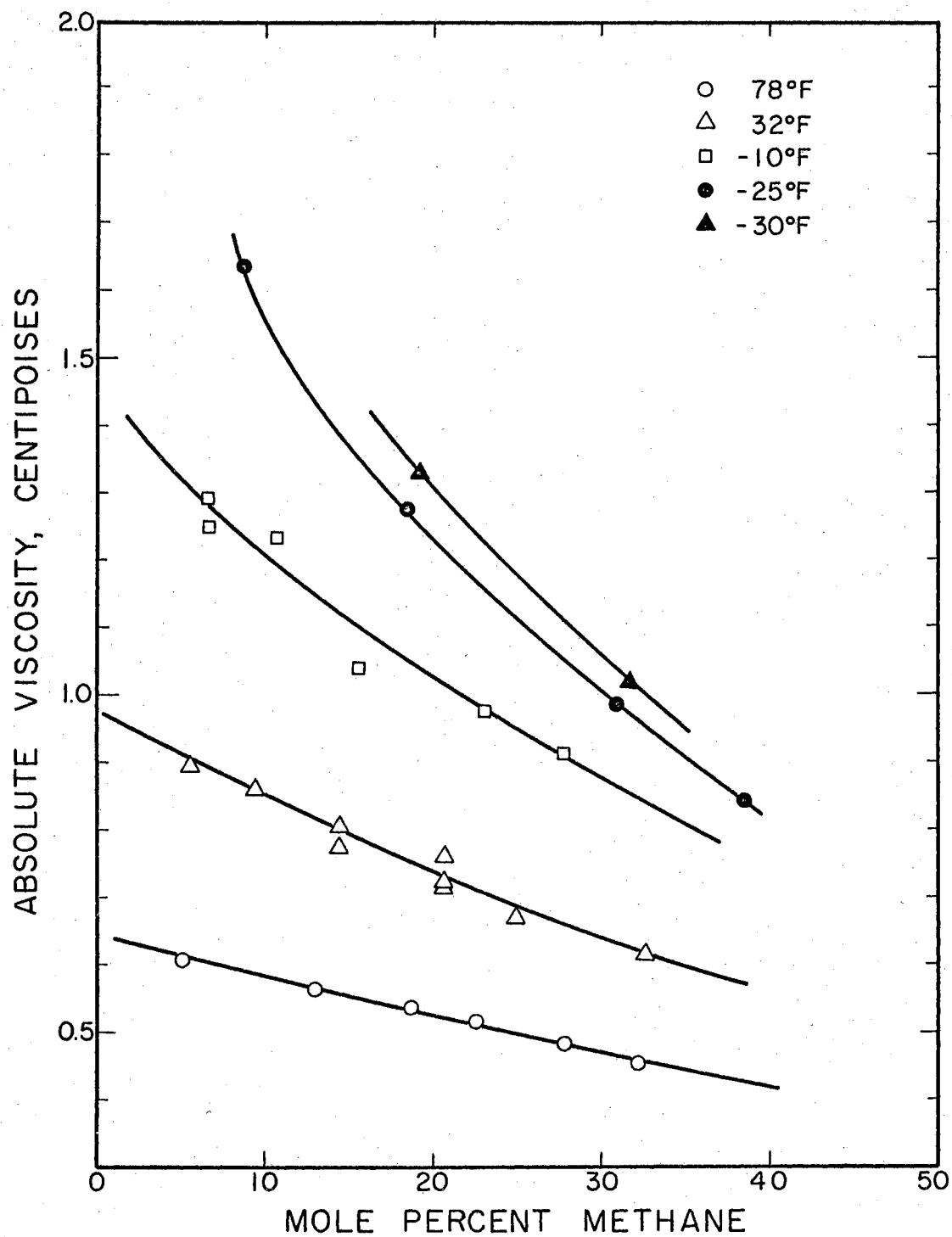


Figure 9. Absolute Viscosity of Methane-Nonane Bubble Point Mixtures as a Function of Composition

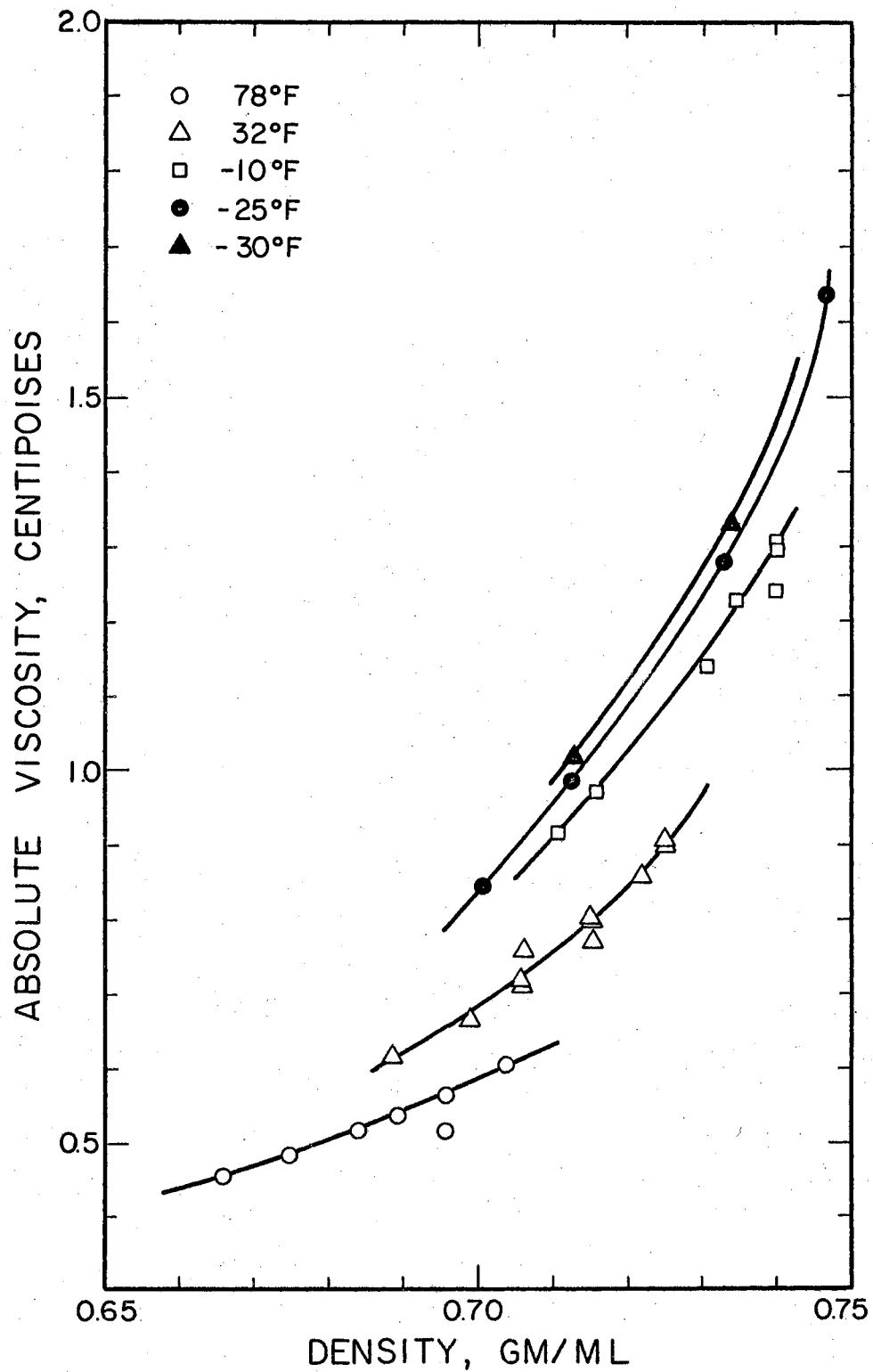


Figure 10. Absolute Viscosity of Methane-Nonane Bubble Point Mixtures as a Function of Density

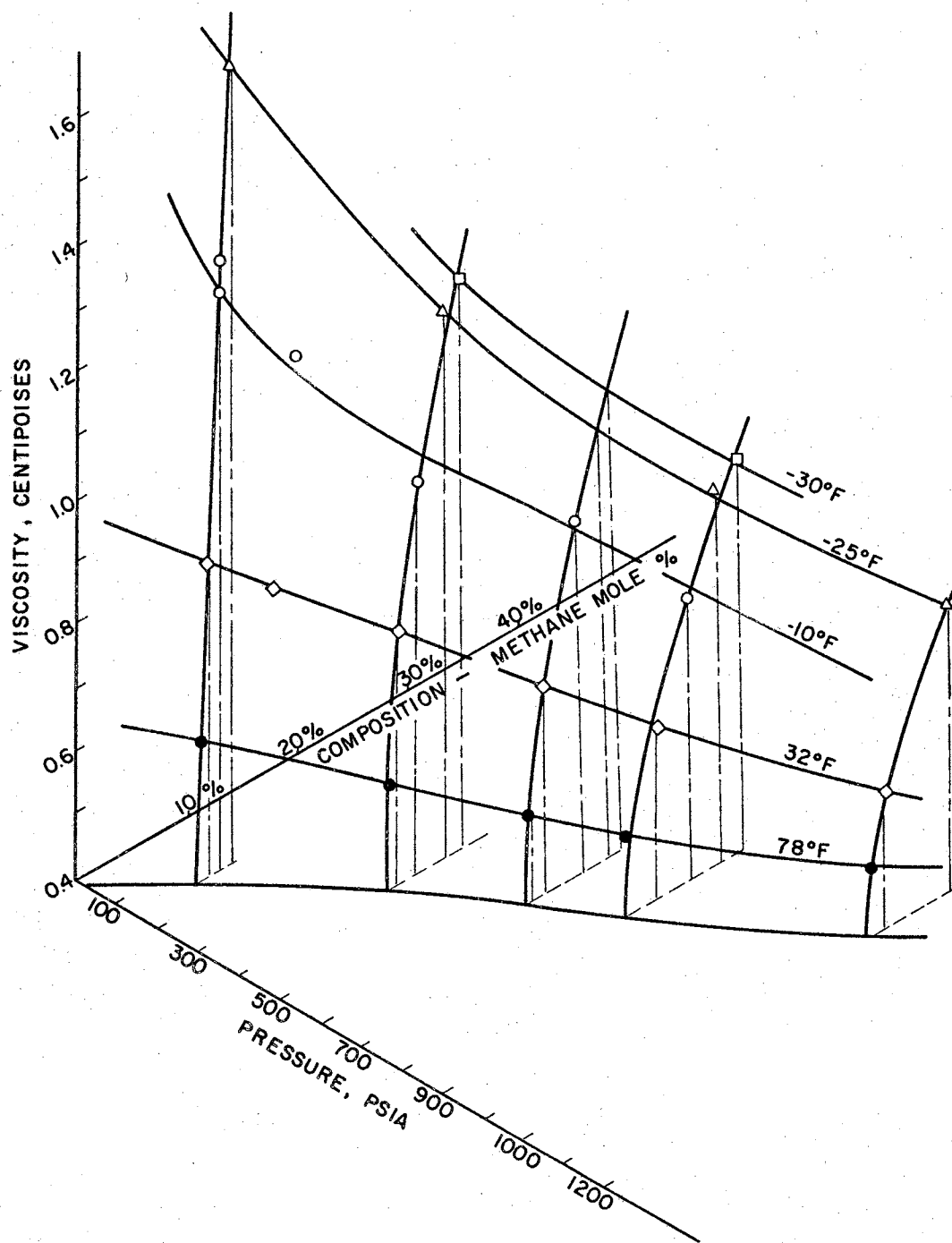


Figure 11. Absolute Viscosity of Methane-Nonane Bubble Point Mixtures as a Function of Composition and Pressure

Surface-Tension Viscosity Correlation

In order to correlate absolute viscosity and surface tension, a method attributed to Pelofsky (22) was employed. Pelofsky found that a straight line resulted when the logarithm of surface tension was plotted against reciprocal viscosity. The natural logarithm of surface tension interpolated from Deam's data (8) and pure nonane data from API Project 44 (26) was plotted against reciprocal absolute viscosity for pure nonane and three compositions of methane and nonane in Figure 12. For a constant composition, the data points appear to fall in a straight line.

Coefficients A_0 and A_1 for the first degree polynomial

$$\ln \gamma = A_0 + \frac{A_1}{\mu}$$

were determined by applying a least squares analysis to the data. IBM 1620 facilities at Oklahoma State University were employed for this operation. These coefficients are presented in Table II. As the percentage of methane in the liquid mixture increased the slope of the line (A_1) became less steep. Also, the intersection with the $\ln \gamma$ axis decreased with increasing percentage of methane in the mixture.

In order to further study the Pelofsky correlation method on constant composition data, viscosity data of Carmichael and associates(6) and surface tensions calculated by Deam's Parachor method (8) for the methane-butane system were analyzed in a manner similar to that of the methane-nonane system. These data are presented in Figure 13 and the coefficients are presented in Table II. For a mixture

of 0.394 mole percent methane in the liquid mixture, the $\ln \gamma$ versus $\frac{1}{\mu}$ plot showed a straight line relationship. Although further investigation on additional data would be required to substantiate the application of the Pelofsky correlation to liquid mixtures, the analysis conducted on the methane-nonane and methane-butane systems indicates that the correlation warrants further investigation.

TABLE II
LEAST SQUARES ANALYSIS FOR SURFACE
TENSION-VISCOSITY CORRELATION

Components Mole per cent	\ln Intercept	A_1 Slope	F-Test
Pure C ₉	3.48464	-0.25617	0.00000
0.1 C ₁ -0.9 C ₉	3.30841	-0.22348	0.00002
0.2 C ₁ -0.8 C ₉	3.11899	-0.23182	0.00005
0.3 C ₁ -0.7 C ₇	2.90329	-0.24024	0.00012
Pure C ₄	3.11013	-0.17305	0.0000
0.394 C ₁ -0.606 C ₄	3.11013	-0.00087	0.00000

Note: These values of F indicate the points show no deviation from the fitted curve for probability levels up to 99%.

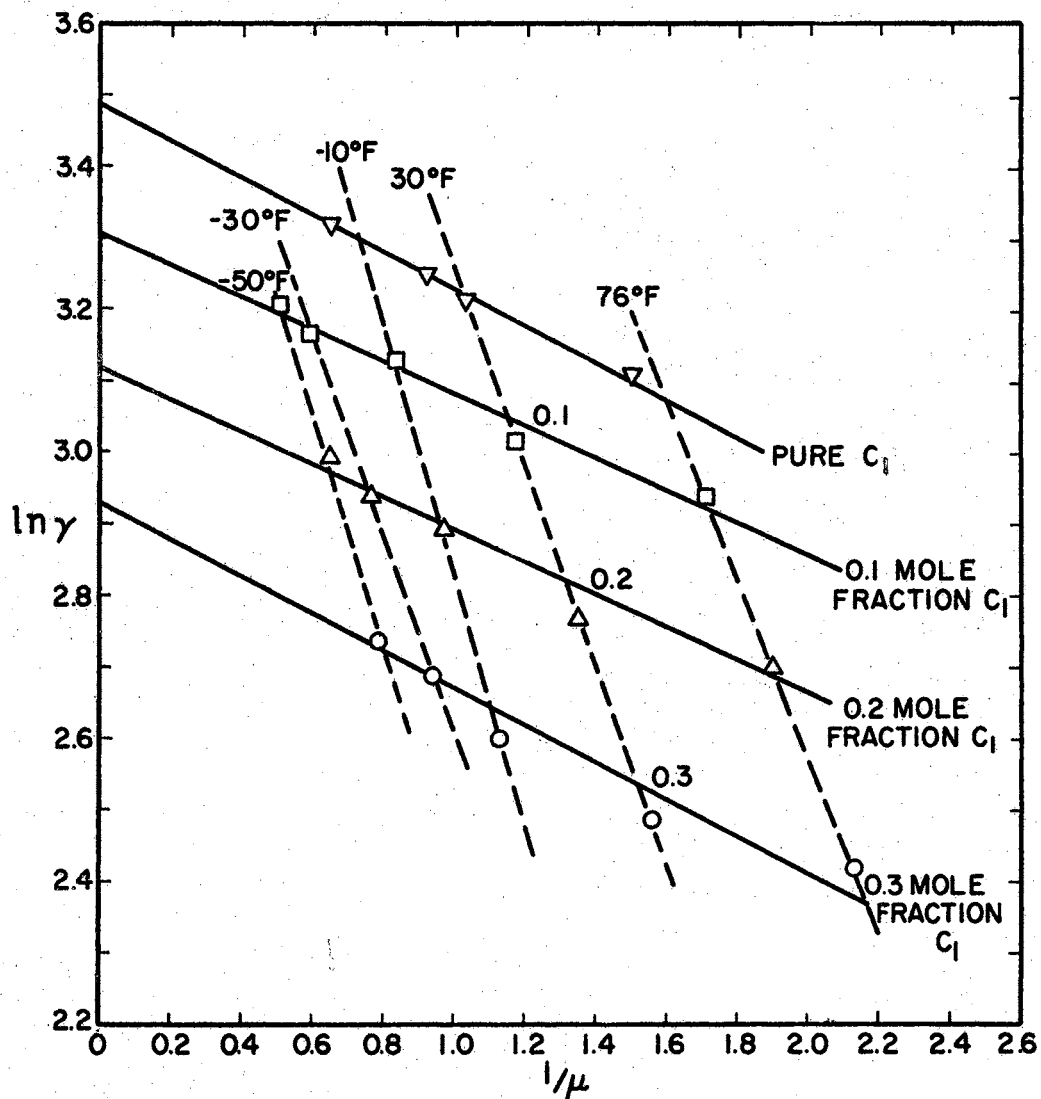


Figure 12. Logarithm of Surface Tension as a Function of Reciprocal Viscosity for Methane-Nonane Mixtures

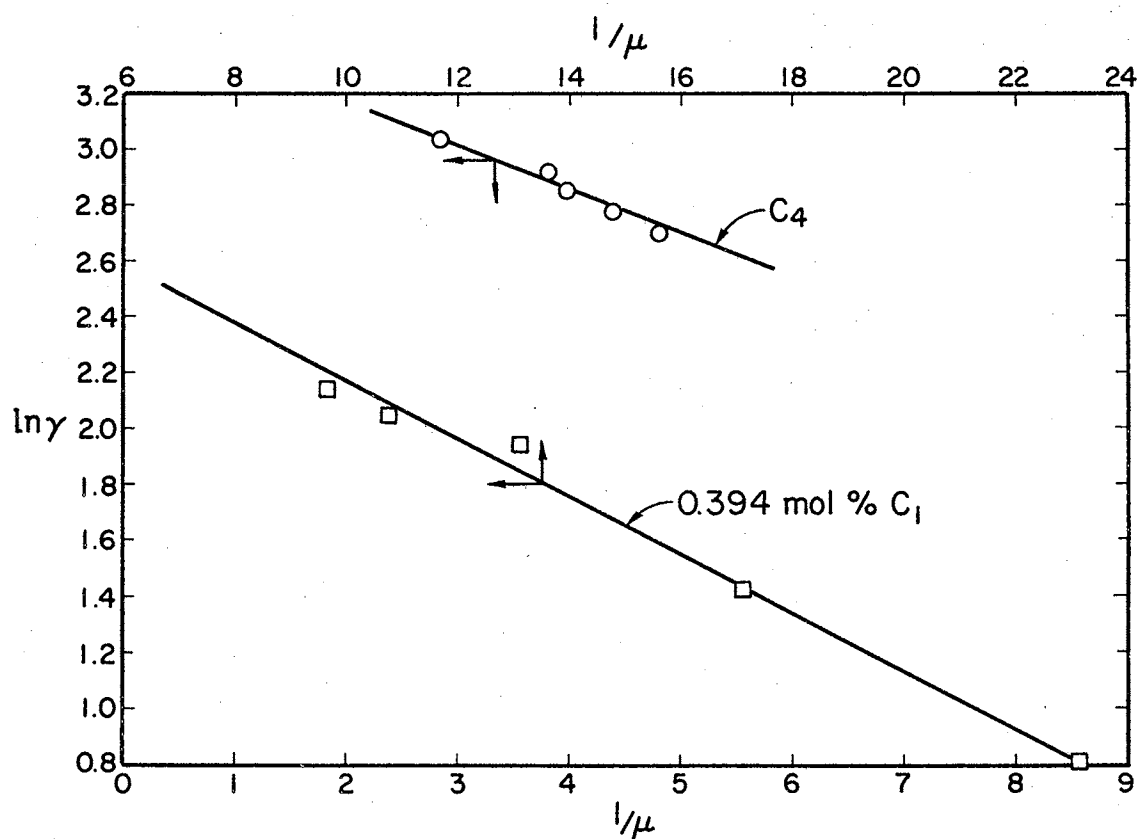


Figure 13. Logarithm of Surface Tension as a Function of Reciprocal Viscosity for Methane-Butane Mixtures

CHAPTER VI

CONCLUSIONS AND RECOMMENDATIONS

Conclusions

The first two objectives of this investigation as presented in Chapter I were the construction of an apparatus suitable for obtaining kinematic viscosity measurements for binary hydrocarbon mixtures and the obtaining of such data. The equipment constructed and used in this investigation allowed measurement of kinematic viscosities for a binary hydrocarbon mixture over a temperature range of -30° F to 78° F and pressures up to 1200 psia. Data obtained by using the equipment constructed were consistent and reproducible (see Figure 6 and Table I) and thus satisfied the second objective presented in Chapter I.

Because the equipment did operate successfully, there were some techniques and methods employed which also may be considered successful. The successful operation of the observation port assemblies provided a basis for the design of such assemblies in the future. Also, preliminary tests of the viscometers used in this investigation showed that repeated measurements on a liquid sample in a wet viscometer will yield consistent flow times.

The third objective of the investigation (comparison of

the behavior of absolute viscosity as temperature, pressure, and composition vary) was achieved and is illustrated by Figures 7 - 11. Conclusions reached concerning the behavior of absolute viscosity for the methane-nonane bubble point mixtures are:

1. For a given isotherm, absolute viscosity increased as pressure decreased. In fact, the viscosity increased more rapidly as pressure was decreased as lower temperature isotherms were studied.

2. For a given isotherm, absolute viscosity decreased as the percentage of methane in the liquid mixture was increased.

3. For a given pressure, absolute viscosity decreased as the temperature increased. When progressively lower pressures were studied, the rate of decrease of viscosity was greater as temperature increased.

4. On a three dimensional plot of composition, pressure and viscosity, the following trends were indicated:

- a) An increase in methane composition at constant pressure yields an increase in absolute viscosity and a decrease in system temperature.

- b) An increase in pressure at a constant composition yields a decrease in system

viscosity and an increase in temperature.

c) The influences of temperature on viscosity were greater than either pressure or composition changes.

5. Comparison of absolute viscosity changes with density showed that viscosity increased very rapidly as the density of the liquid mixture increased.

6. The logarithm of surface tension plotted against reciprocal viscosity for constant composition mixtures produced straight lines. Experimental methane-nonane data and methane-butane mixture data from the literature produced the same trend in results.

Recommendations

Even though the equipment as built seemed to work satisfactorily, there are improvements which could be made to facilitate obtaining kinematic viscosity measurements.

These changes are:

1. Change the Heise gauge connection from the present location in the pressure line to a line leading directly from the pressure cell. This modification would eliminate any pressure lines between the pressure cell and the gauge. Time lag between a pressure change and a

- response on the gauge would be minimized.
2. Lengthen the liquid injector tube to allow the viscometer to hang lower in the pressure cell. This improvement would permit the lines on the viscometer bulb to be seen more easily.
 3. Improve the method of illuminating the viscometer inside the pressure cell. This improvement would also allow easier observation of the lines of the viscometer bulb.
 4. Install rotameters in the inlet and outlet methanol lines of the refrigeration system to allow measurement of the flow of coolant to the temperature bath. Control of the coolant level in the constant temperature bath was one of the major problems in operating the system. Flowmeters would enable the operator to balance inlet and outlet flows.
 5. Install an additional Heise gauge with a range of from 0 psia to 500 psia to permit a more accurate study of viscosity at lower pressures. The present gauge is not graduated in small enough increments to measure pressures for a detailed study at lower pressures. It is in the low pressure region that the greatest viscosity deviations

appear to occur.

Since the viscosity appeared to increase quite sharply with decreasing pressures and temperatures (Figures 7 and 8) other investigations might be undertaken to more closely examine the behavior of bubble-point mixtures at low temperature and pressure conditions. The behavior of the surface tension-viscosity correlation proposed by Pelofsky should be investigated in further studies of mixture viscosities.

NOMENCLATURE

English Letters

A, B	=	constants for interfacial tension-viscosity correlation
C_1, C_2	=	viscometer constants
D	=	capillary tube diameter
F	=	force applied to a fluid
g	=	gravitational constant
H	=	mean hydrostatic head
h	=	Planck's constant
k	=	constant in Poiseuille's law
L	=	capillary tube length
M	=	molecular weight
N	=	Avogadro's number
P	=	pressure
P_c	=	critical pressure
Q	=	volumetric flow rate
R	=	gas constant
r	=	radius of capillary
T	=	temperature
T_c	=	critical temperature
t	=	time
V	=	volume

V	=	molar volume
v	=	velocity
\bar{v}	=	mean velocity
W	=	interaction energy for activation of flow

Greek Letters

α	=	distance through which shearing force acts
δ	=	interfacial tension
Δ	=	a change in a quantity
ϵ	=	correction factor for end effects in capillary
λ	=	distance between adjacent moving layers of molecules
μ	=	dynamic or absolute viscosity
μ^0	=	viscosity at atmospheric pressure and at the reference temperature
ν	=	kinematic viscosity
π	=	3.1415...
ρ	=	density

Subscripts

A	=	arithmetic mean
c	=	critical point property
G	-	geometric mean
i	-	ith component
m	=	mixture
R	=	reduced property
1, 2	=	number of the particular component

A. SELECTED BIBLIOGRAPHY

- (1) Barr, Guy, A Monograph of Viscometry, London: Oxford University Press, 1931.
- (2) Bicher, L. B., and D. L. Katz, Ind. Eng. Chem., 35, (1943), 754-761.
- (3) Bird, R. B., W. E. Stewart, and E. N. Lightfoot, Transport Phenomena, New York: John Wiley and Sons, 1963.
- (4) Brebach, W. J., and George Thodos, Ind. Eng. Chem., 50, (1958), 1095-1100.
- (5) Comings, E. W., and R. S. Egly, Ind. Eng. Chem., 32, (1940), 714-718.
- (6) Carmichael, L. T., Virginia Berry, and B. H. Sage., J. Chem. Eng. Data, 12, (1967), 44-47.
- (7) Cullinan, H. T., Ind. Eng. Chem., 7, (1968), 177-180.
- (8) Deam, J. R., Unpublished Ph.D. dissertation, Oklahoma State University, Stillwater, Oklahoma, 1968.
- (9) Dinsdale, A., and F. Moore, Viscosity and Its Measurement, New York: Reinhold Publishing Corporation, 1962.
- (10) Dolan, J. P., R. T. Ellington, and A. L. Lee, J. Chem. Eng. Data, 9, (1964), 484-487.
- (11) Dolan, J. P., K. E. Starling, A. L. Lee, B. E. Eakin, and R. T. Ellington, J. Chem. Eng. Data, 8, (1963), 396-399.
- (12) Glasstone, S. N., K. Laidler, and H. Eyring, The Theory of Rate Processes, New York: McGraw-Hill Book Company, 1941.
- (13) Gonzalez, M. H., and R. F. Bukacek, to be published as SPB Report 1482, 1967.
- (14) Heric, E. L., and J. G. Brewer, J. Chem. Eng. Data, 12, (1967), 574-583.

- (15) Johnson, J. F., R. L. LeTourneau, and Robert Matteson, Anal. Chem., 24, (1952), 1505-1508.
- (16) Katti, P. K., and M. M. Chaudri, J. Chem. Eng. Data, 9, (1964), 442.
- (17) Kay, W. B., Ind. Eng. Chem., 28, (1936), 1014.
- (18) Lee, A. L., M. H. Gonzalez, and B. E. Eakin, J. Chem. Eng. Data, 11, (1966), 281-287.
- (19) Macedo, P. B., and T. A. Litovitz, J. Chem. Phys., 42, (1965), 245-256.
- (20) Nelson, W. L., Oil Gas J., 50, (1939), 38-39.
- (21) Newton, Isaac S., Philosophiae Naturalis Principia Mathematica, 1st Ed., Book 2, Section IX, 1687.
- (22) Pelofsky, A. H., J. Chem. Eng. Data, 11, (1966), 394-397.
- (23) Perry, J. H., Chemical Engineer's Handbook, Third Edition. New York" McGraw-Hill Book Company, 1950.
- (24) Poiseuille, J. L., Compte Rendus, 11, 961 and 1041, 1840.
- (25) Reamer, H. H., G. Cokelet, and B. H. Sage, Anal. Chem., 31, (1959), 1422-1428.
- (26) Rossini, F., et al, "Selected Values of Properties of Hydrocarbons and Related Compounds," API Research Project 44, American Petroleum Institute, New York.
- (27) Sage, B. H., and W. N. Lacey, "Thermodynamic Properties of the Lighter Paraffin Hydrocarbons and Nitrogen," API Research Project 37, American Petroleum Institute, New York, 1950.
- (28) Schonhorn, Harold, J. Chem. Eng. Data, 12, (1967), 524-525.
- (29) Shipman, L. M., and J. P. Kohn, J. Chem. Eng. Data, 11, (1966), 176-180.
- (30) Smith, A. S., and G. G. Brown, Ind. Eng. Chem., 35, (1943), 705-711.
- (31) Starling, K. E., B. E. Eakin, and R. T. Ellington, AICHE J., 6, (1960), 438-442.

- (32) Uyehara, O. A., and K. M. Watson, Nat'l. Petrol. News, Tech. Sect., (Oct. 4, 1944), R764.
- (33) Van Wazer, J. R., J. W. Lyons, K. Y. Kim, and R. E. Colwell, Viscosity and Flow Measurement, New York: Interscience Publishers, 1963.
- (34) Weber, J. H., Absorption Literature Survey (NGPA), (Sept. 3, 1964), 77.
- (35) Zeitfuchs, E. H., Oil Gas J., 44, (Jan. 12, 1946), 99.

APPENDIX A

HEISE GAUGE CALIBRATION

The calibration of 3000 psi Heise gauge No. 51054 is given in Table III. The calibration was performed by A. K. Arnett on August 28, 1967, with dead weight gauges certified by the Bureau of Standards to have an average accuracy of within one part in 35,000. Calibration procedures were performed at 70° F.

TABLE III

HEISE GAUGE CALIBRATION

Dead Weight Reading	Deviation* from Dead Weight on Heise Gauge
150	-
300	-
450	-
600	-
750	-
900	-
1050	-
1200	-
1350	-
1500	-
1650	-
1800	-
1950	-
2100	-
2250	-
2400	-
2550	-
2700	-
2850	-
3000	-

*Corrections are indicated where error is 3 psi or more.

APPENDIX B

MEASUREMENT REPRODUCIBILITY

In order to simplify the experimental measuring procedure, repeated measurements were conducted for a set of temperature and pressure conditions on the same liquid sample. To investigate the reproducibility of data obtained by this procedure, distilled water and n-nonane viscosities were measured at atmospheric pressure and room temperature using several measurements on one sample and one measurement on each of several liquid samples. The methods used, data obtained, results of the investigation and required viscometer calibrations are presented in this appendix.

Distilled water was introduced to the reservoir of a Zeitfuchs style capillary viscometer so that the water level corresponded to the hairlines scribed on the glass wall. Suction was applied to the capillary to initiate the flow of water through the capillary. The time required for the water to fill the measuring bulb was recorded. After the measurement was completed, suction was applied to the reservoir end of the viscometer, the liquid was forced back into the reservoir, and a new measuring run was initiated. Times required and tube conditions are given in Table IV. The viscometer used during the study had a reported cell constant

of 0.01.

Examination of the data obtained indicated that repeated measurements on the same sample were, in fact, reproducible and that times recorded for dry bulb measurements showed very little difference when compared to times for wet bulb measurements. For purposes of this viscosity study of methane-n-nonane bubble point mixtures, a procedure of repeated measurements could be used with confidence providing the viscometer was calibrated for repeated operation.

TABLE IV
REPRODUCIBILITY STUDY

Materials and Conditions	Temp (°F)	Time (Sec)	% Dev.	Measuring Bulb Condition
Distilled Water Atm. Press	76	81.6	+0.61	Dry Bulb (All measurements after the first were conducted with a wet measuring bulb.)
	76	81.0	-0.12	
	76	81.0	-0.12	
	76	81.0	-0.12	
	76	81.0	-0.12	
	76	81.0	0	
	76	81.1	0	
	76	81.1	0	
	76	81.0	-0.12	
	Avg.	81.1		
Distilled Water Chm. Press	78	81.0	-0.37	Dry Bulb
	78	81.7	+0.49	Wet Bulb
	78	81.5	+0.25	Wet Bulb
	78	81.0	-0.37	Wet Bulb
	Avg.	81.3		
N-Nonane Atm. Press	78	82.8	-1.15	Dry Bulb
	78	84.0	+0.30	Wet Bulb
	78	84.0	+0.30	Wet Bulb
	78	84.2	+0.54	Wet Bulb
	Avg.	83.75		
Distilled Water Atm. Press	74	82.03	+0.78	All runs conducted on a wet measuring bulb.
	76	82.35	+1.18	
	77	83.35	+2.41	
	77	83.94	+0.67	
	77	80.67	-0.88	
	77	80.43	-1.18	
	77	80.21	-1.45	
	77	80.29	-1.35	
	77	80.25	-1.40	
	77	80.35	-1.27	
		Avg.	81.39	

TABLE IV (continued)
REPRODUCIBILITY STUDY

Materials and Conditions	Temp (°F)	Time (Sec)	% Dev.	Measuring Bulb Condition
Distilled Water	77	83.435	+2.53	Dry Bulb
	77	80.77	-0.98	Wet Bulb
Atm. Press	77	81.23	-0.42	
	77	81.19	-0.46	
	77	81.23	-0.42	
	Avg.	81.57		
Distilled Water	77	81.14	-1.45	Dry Bulb
	77	81.98	-1.64	Dry Bulb
Atm. Press	77	84.96	+3.2	Dry Bulb
	77	83.29	+1.16	Dry Bulb
	77	81.19	-1.38	Dry Bulb
	77	80.85	-3.01	Dry Bulb
	77	81.57	-0.92	Wet Bulb
	77	80.58	-2.13	Wet Bulb
	77	84.13	+2.18	Wet Bulb
	77	81.10	-1.50	Wet Bulb
	77	84.91	+3.14	Wet Bulb
Avg.	82.33			
Distilled Water	76	81.55	+1.39	Wet Bulb
	76	80.12	-0.39	Wet Bulb
Atm. Press	76	80.36	-0.09	Wet Bulb
	76	80.68	+0.31	Wet Bulb
	76	80.45	+0.02	Wet Bulb
	76	79.65	-0.97	Dry Tube
	76	79.43	-1.25	Dry Tube
	76	81.23	+1.00	Dry Tube
	Avg.	80.43		
Nonane	77	85.45	-0.65	Wet Bulb
	77	84.54	-1.71	Wet Bulb
Atm. Press	77	85.20	-0.94	Wet Bulb
	77	86.20	+0.22	Wet Bulb
	77	85.58	-0.50	Wet Bulb
	77	85.94	-0.08	Wet Bulb
	77	87.51	+1.75	Dry Bulb
	77	87.16	+1.34	Wet Bulb
	77	87.65	+1.64	Wet Bulb
	77	87.42	+2.59	Wet Bulb
	77	88.24	+2.58	Wet Bulb
	77	86.81	-0.81	Dry Bulb
	77	83.44	-2.98	Dry Bulb
	77	83.04	-3.45	Dry Bulb
	Avg.	86.01		

TABLE IV (Continued)
REPRODUCIBILITY STUDY

Material and Conditions	Temp (°F)	Time (Sec)	% Dev	Measuring Bulb Condition
Nonane	76	84.41	-0.31	Dry Bulb
	76	85.65	+1.05	Dry Bulb
Atm. Press	76	84.76	+0.11	Dry Bulb
	76	84.63	-0.05	Dry Bulb
	76	84.62	-0.06	Dry Bulb
	76	84.85	+0.21	Dry Bulb
	76	84.49	-0.21	Dry Bulb
	76	84.17	-0.59	Dry Bulb
	76	84.36	-0.37	Dry Bulb
	76	84.82	+0.18	Dry Bulb
	Avg.	84.67		
Distilled Water	77	90.11	+5.33	Dry Bulb
	77	87.73	+2.55	Dry Bulb
	77	83.70	-2.16	Dry Bulb
	77	83.27	-2.66	Dry Bulb
	77	83.72	-2.14	Dry Bulb
	77	83.56	-2.33	Dry Bulb
Avg.	85.55			
Distilled Water	77	83.84	-0.64	Wet Bulb
	77	84.15	-0.27	Wet Bulb
Atm. Press	77	84.74	+0.43	Wet Bulb
	77	84.32	-0.07	Wet Bulb
	77	84.55	-0.03	Wet Bulb
	77	84.83	+0.53	Wet Bulb
	77	84.43	+0.06	Wet Bulb
	Avg.	84.38		

APPENDIX C

VISCOMETER CALIBRATION

Two Zeitfuchs C-50 style viscometers were calibrated at atmospheric pressure and at room temperature. Literature values for the viscosity of distilled water were obtained from Perry's(23). The procedure for the calibration was to obtain data by repeated measurement of a sample as practiced in the reproducibility study presented in Appendix B. Table V presents the data taken during the calibration and Table VI shows the calculated cell constants.

TABLE V
VISCOMETER CALIBRATION

Visc. No.	Run	Temp.	Time (Sec.)	Standard Dev.
U 2893	1	77°F	84.4	S = 0.476 3S = 1.328sec 2S = .932
	2	77	81.6	
	3	77	83.0	
	4	77	81.0	
	5	77	80.4	
	6	77	80.4	
	7	77	80.3	
	8	77	79.8	
	9	77	82.0	
	10	77	79.7	
	11	77	80.0	
			Avg. <u>81.4</u>	
U 3820	1	78°F	265.14*	S = 0.59 3S = 1.77 sec 2S = 8
	2	79	263.3*	
	3	78	251.5	
	4	78	249.4	
	5	78	250.8	
	6	78	248.8	
	7	78	248.8	
	8	78	248.3	
			Avg. <u>249.6</u>	
U 3502	1	78°F	262.9	S = 0.61 3S = 1.83 sec
	2	78	264.0	
	3	78	262.2	
	4	78	260.8	
	5	78	264.8	
	6	78	261.4	
	7	78	264.2	
			Avg. <u>262.9</u>	

*Times recorded for a dry viscometer.

TABLE VI

CALCULATED VISCOMETER CONSTANTS

Viscometer No.	Avg. Time (Sec)	Constant	
		Reported	Calculated
U 2893	81.14	0.01	0.011
U 3820	249.6	0.003	0.0035
U 3502	262.9	0.003	0.0034

APPENDIX D

EXPERIMENTAL AND CALCULATED DATA

TABLE VII
EXPERIMENTAL FLOW TIMES

Series Visc. No. Temp (°F) Press (PSIA)	Run	Time (Sec)	% Dev.
1 U2893 78°F 150 PSIA	1	78.6	+0.25
	2	78.2	-0.25
	3	78.4	0
	4	78.4	0
	Avg.	<u>78.4</u>	
2 U2893 78°F 150 PSIA	1	80.8	+3.3
	2	75.4	-3.6
	3	78.0	-0.26
	4	76.0	-2.8
	5	80.4	2.8
	6	78.8	+0.76
Avg.	<u>78.2</u>		
3 U2893 78°F 400 PSIA	1	73.7	Equilibrium
	2	72.4	not
	3	72.4	Attained
	4	70.2	-0.7
	5	71.4	+0.99
	6	71.5	+0.28
	7	70.4	-0.42
	8	71.0	+0.42
	9	70.1	-0.56
	10	70.2	-0.7
Avg.	<u>70.7</u>		
4 U2893 78°F 750 PSIA	1	71.4	+3.5
	2	71.4	+3.5
	3	70.3	+1.9
	4	70.2	+1.7
	5	69.0	0.0
	6	68.8	-0.29
	7	71.7	+3.8
	8	69.6	+0.87
	9	67.4	-2.3
	10	68.1	-1.3
Avg.	<u>69.0</u>		

TABLE VII (continued)

EXPERIMENTAL FLOW TIMES

Series Visc. No. Temp (°F) Press (PSIA)	Run	Time (Sec)	% Dev.
5 U2893 78°F 1000 PSIA	1	68.7	+5.2
	2	66.4	+1.7
	3	65.4	+0.16
	4	65.4	+0.16
	5	65.4	+0.16
	6	64.5	-1.20
	7	64.5	-1.20
	8	65.4	+0.16
	Avg.	<u>65.3</u>	
6 U2893 78°F 1200 PSIA	1	64.6	+4.2
	2	61.0	-1.6
	3	61.6	-0.64
	4	62.3	+0.48
	5	62.6	+0.97
	6	62.4	+0.65
	7	75.3	Entrained Nonane into the System
	8	74.2	
	9	74.0	
	10	67.2	
	Avg.	<u>62.0</u>	
7 U2893 78°F 400 PSIA	1	74.0	+0.27
	2	73.8	0
	3	73.8	0
	4	73.8	0
	5	73.8	0
	6	73.8	0
	7	73.8	0
	Avg.	<u>73.8</u>	
8 U2893 78°F 600 PSIA	1	71.9	+1.55
	2	76.4	-
	3	70.7	-0.14
	4	70.8	0.0
	5	70.6	-0.28
	6	70.8	0.0
	7	71.0	+0.28
	8	70.4	-0.56
	9	70.3	-0.71
	Avg.	<u>70.8</u>	

TABLE VII (continued)

EXPERIMENTAL FLOW TIMES

Series Visc. No. Temp (°F) Press (PSIA)	Run	Time (Sec)	% Dev.
9 U2893 -10°F 150 PSIA	1	155.7	-0.19
	2	155.3	-0.45
	3	155.5	-0.32
	4	157.4	+0.90
	5	Entrained	
	6	Nonane	
	Avg.	<u>155.97</u>	
10 U2893 -10°F 600 PSIA	1	123.8	+0.40
	2	123.3	0.0
	3	123.2	-0.08
	4	123.2	-0.08
	5	123.8	+0.40
	6	<u>122.8</u>	-0.40
	Avg.	<u>123.3</u>	
11 U2893 -10°F 150 PSIA	1	160.8	+0.06
	2	161.0	+0.19
	3	160.2	-0.31
	4	160.2	-0.31
	5	161.0	+0.19
	6	<u>161.0</u>	+0.19
	Avg.	<u>160.7</u>	
12 U2893 -10°F 150 PSIA	1	106.4	System
	2	104.0	Had Not
	3	104.4	Attained
	4	101.0	Equilibrium
	5	101.0	+1.42
	6	99.7	+1.11
	7	98.4	-0.21
	8	98.0	-0.61
	9	98.2	-0.40
	10	<u>98.6</u>	0.0
	Avg.	<u>98.6</u>	

TABLE VII (continued)

EXPERIMENTAL FLOW TIMES

Series Visc. No. Temp (°F) Press (PSIA)	Run	Time (Sec)	% Dev.
13 U2893 32°F 150 PSIA	1	125.4	Equilibrium
	2	126.6	Had Not
	3	124.2	Been
	4	110.6	Achieved
	5	114.0	0.0
	6	113.6	-0.35
	7	114.0	0.0
	8	114.0	0.0
	9	114.0	0.0
	10	113.4	-0.53
	11	114.6	+0.53
	Avg.	<u>114.0</u>	
14 U2893 -10°F 750 PSIA	1	117.6	+0.34
	2	116.5	-0.60
	3	117.5	+0.26
	4	116.3	-0.77
	5	117.4	+0.17
	6	117.7	+0.43
	Avg.	<u>117.2</u>	
15 U2893 -10°F 400 PSIA	1	128.2	-1.08
	2	128.8	-0.62
	3	130.8	+0.92
	4	131.2	+1.23
	5	129.8	+0.15
	6	128.4	-0.93
	7	129.7	+0.08
	8	130.2	+0.46
	Avg.	<u>129.6</u>	
16 U2893 -10°F 150 PSIA	1	158.2	-0.63
	2	159.2	0.0
	3	159.4	+0.125
	4	159.6	+0.255
	5	159.4	+0.125
	Avg.	<u>159.2</u>	

TABLE VII (continued)

EXPERIMENTAL FLOW TIMES

Series Visc. No. Temp (°F) Press (PSIA)	Run	Time (Sec)	% Dev.
17 U2893 32°F 750 PSIA	1	88.2	+1.9
	2	87.8	+0.30
	3	88.0	+0.54
	4	87.2	-0.39
	5	87.6	+0.07
	6	87.0	-0.62
	7	87.0	-0.62
	Avg.	87.54	
18 U2893 32°F 400 PSIA	1	98.0	0.0
	2	97.4	-0.58
	3	97.4	-0.58
	4	98.2	+0.20
	5	98.4	+0.41
	6	98.4	+0.41
	Avg.	97.97	
19 U2893 32°F 1000 PSIA	1	82.0	+0.28
	2	81.0	-0.94
	3	81.7	0.0
	4	82.6	+1.02
	5	82.3	+0.57
	6	81.0	-0.94
	Avg.	81.77	
20 U2893 32°F 600 PSIA	1	92.8	+0.43
	2	92.0	-0.43
	3	92.6	+0.22
	4	92.0	-0.43
	5	92.6	+0.22
	Avg.	92.4	
21	(Incomplete Run)		
22 U2893 32°F 150 PSIA	1	113.6	+1.16
	2	111.5	-0.71
	3	112.5	+0.18
	4	112.3	0.0
	5	112.2	-0.09
	6	111.7	-0.53
	Avg.	112.3	

TABLE VII (continued)

EXPERIMENTAL FLOW TIMES

Series Visc. No. Temp (°F) Press (PSIA)	Run	Time (Sec)	% Dev.
23 U2893 32°F 250 PSIA	1	109.5	+0.92
	2	107.6	-1.75
	3	107.8	-1.55
	4	108.2	-0.27
	5	109.5	+0.92
	Avg.	108.5	
24 U2893 32°F 400 PSIA	1	103.3	+0.39
	2	102.6	-0.29
	3	102.8	-0.097
	4	103.6	+0.68
	5	102.4	-0.48
	Avg.	102.9	
25 U2893 32°F 400 PSIA	1	102.2	0.0
	2	102.2	0.0
	3	102.2	0.0
	4	102.2	0.0
	5	102.2	0.0
	Avg.	102.2	
26 U2893 32°F 600 PSIA	1	93.0	0.00
	2	92.8	-0.21
	3	92.8	-0.21
	4	92.8	-0.21
	5	92.6	-0.43
	6	93.6	+0.64
	7	93.2	+0.21
	8	93.8	+0.78
	Avg.	93.07	
27 U2893 32°F 400 PSIA	1	101.6	-0.37
	2	101.8	-0.18
	3	102.6	+0.61
	4	102.4	+0.41
	5	101.5	-0.47
	Avg.	101.98	
28 U2893 -10°F 250 PSIA	1	152.0	-0.52
	2	153.0	+0.13
	3	153.0	+0.13
	4	153.0	+0.13
	5	153.0	+0.13
	Avg.	152.8	

TABLE VII (continued)

EXPERIMENTAL FLOW TIMES

Series Visc. No. Temp (°F) Press (PSIA)	Run	Time (Sec)	% Dev.
29 U2893 -25°F 150 PSIA	1	198.4	-0.60
	2	200.3	+0.35
	3	199.8	+0.10
	4	200.6	+0.50
	5	198.0	-0.80
	6	200.6	+0.50
	Avg.	<u>199.6</u>	
30	(Incomplete Run)		
31 U2893 -25°F 400 PSIA 400 PSIA	1	158.8	+0.25
	2	157.8	-0.38
	3	158.4	0.0
	4	158.2	-0.13
	5	158.8	+0.25
	Avg.	<u>158.4</u>	
32 U2893 -30°F 400 PSIA	1	164.6	+0.18
	2	165.0	+0.42
	3	164.0	-0.18
	4	164.0	-0.18
	5	164.0	-0.18
	Avg.	<u>164.3</u>	
33 U2893 -25°F 750 PSIA	1	126.0	+0.08
	2	125.0	-0.71
	3	126.8	+0.71
	4	125.4	-0.40
	5	126.4	+0.40
	Avg.	<u>125.9</u>	
34 U2893 -30°F 750 PSIA	1	130.2	+0.08
	2	130.2	+0.08
	3	129.8	-0.23
	4	130.0	-0.08
	5	130.2	+0.08
	Avg.	<u>130.1</u>	
35 U2893 -25°F 1000 PSIA	1	109.8	-0.25
	2	110.4	+0.29
	3	110.2	+0.11
	4	109.9	-0.16
	5	110.1	+0.02
	Avg.	<u>110.08</u>	

APPENDIX E

ANALYSIS OF ERROR METHOD AND EVALUATION

The method of calculating the most probable value of error as a result of experimental measurements has been presented by J. R. Deam(8). Experimental error is determined by combination of the errors attributable to each term of the basic viscosity equation used in this study.

$$\mu = c, t \rho \quad (21)$$

The errors due to each quantity can be defined as follows:

$$\mu_c = \frac{\partial \mu}{\partial c} \delta_c = t \rho \delta_c \quad (22a)$$

$$\mu_t = \frac{\partial \mu}{\partial t} \delta_t = c \rho \delta_t \quad (22b)$$

$$\mu_\rho = \frac{\partial \mu}{\partial \rho} \delta_\rho = c t \delta_\rho \quad (22c)$$

where δ_c , δ_t and δ_ρ are uncertainties in each of the quantities.

Total error is defined as follows.

$$\Delta \mu = \sqrt{(\mu_c)^2 + (\mu_t)^2 + (\mu_\rho)^2} \quad (23)$$

Differentiation of equation 21 and substitution into equation 23 yields the following expression for total error.

$$\Delta \mu = \sqrt{\left(\frac{\delta c}{c}\right)^2 + \left(\frac{\delta t}{t}\right)^2 + \left(\frac{\delta \rho}{\rho}\right)^2} \quad (24)$$

The only term of equation 21 which is evaluated experimentally is time, t, which is a function of pressure, temperature, and composition.

$$t = f(T, P, X)$$

It was pointed out earlier that equilibrium conditions were

considered achieved when a consistent set of flow times was achieved for a set of operating conditions. (See Chapter IV) Therefore, the deviations presented previously in Table VII serve only to express consistency of flow times and not accuracy of the measurements. A more representative value of the deviation in time (t) can be determined from consideration of measurements taken on separate samples but at the same set of temperature and pressure conditions.

<u>Temp. F</u>	<u>Press, PSIA</u>	<u>Avg. % Deviation</u>
78	150	1.81
78	400	4.3
32	150	0.75
32	400	1.62
32	600	3.6
-10	150	<u>2.1</u>
		Avg. 2.36

Therefore, in the evaluation of experimental error, the average per cent deviation will be used for the value of M_t .

There is no error associated with the constant of equation 21. The viscometer is designed to eliminate any errors in filling the instrument (35).

Shipment and Kohn (29) claim that their data for the methane-nonane system is reproducible to within 0.1%. However, their estimated error for the measurements they presented was about $\pm 1\%$.

Evaluation of the total percent error is given below.

Values used for the uncertainties of equation 24 are the following:

$$\delta\tau = 0.0236$$

$$\delta\rho = 0.01$$

$$\delta c = 0$$

Dividing the total error, $\Delta\mu$, of equation 24 by the viscosity being measured, μ , yields the following result for percent error.

$$\frac{\Delta\mu}{\mu} = \sqrt{(0.0236)^2 + (0.01)^2 + (0)} \quad (25)$$

Therefore,

$$\frac{\Delta\mu}{\mu} = 0.0256$$

or an average percent error of 2.56%.

Using a maximum uncertainty for measurement of 4.3%, the maximum resulting percent error in viscosity is 4.4%. The maximum deviations occurred during the initial stages of the experimental work. After experimental technique had been refined the percent error decreased. The trend indicated that the value of 2.56% for the average error is probably representative of the accuracy of the overall experimental results.

VITA

Stuart Edward Bennett

Candidate for the Degree of
Master of Science

Thesis: MEASUREMENT OF VISCOSITIES OF SATURATED METHANE
NONANE LIQUID MIXTURES AT ELEVATED PRESSURES WITH
A CAPILLARY VISCOMETER

Major Field: Chemical Engineering

Biographical:

Personal Data: Born in Longmont, Colorado, January 21,
1944, to Edward E. and Jeannette E. Bennett

Education: Attended elementary school in Cactus,
Texas, and Bartlesville, Oklahoma; graduated in
1962 from College High School in Bartlesville,
Oklahoma; received the Professional degree of
Petroleum Refining Engineer from the Colorado
School of Mines, Golden, Colorado, June 7, 1966;
attended the University of Illinois at Champaign,
Illinois, from September of 1966 through January
of 1967; completed requirements for the Master of
Science in Chemical Engineering at Oklahoma State
University, Stillwater, Oklahoma, in August, 1969.

Professional Experience: Employed by Phillips
Petroleum Company, Bartlesville, Oklahoma, as a
draftsman and process development engineer during
the summers of 1964 and 1965, respectively; em-
ployed as a process engineer by Shell Chemical
Company, Torrance, California, during the summer
of 1966; currently employed by the Chemplex
Company of Rolling Meadows, Illinois, in polymer
development.

Membership in Scholarly or Professional Societies:
Tau Beta Pi, Sigma Gamma Epsilon, member of the
American Institute of Chemical Engineers.